pd.maguire@ulster.ac.uk

Online Low Temperature Plasma Seminar

July 2021

Multiple phases: charged droplets, colloids and solids in a low temperature atmospheric pressure plasma

Paul Maguire

Ulster University

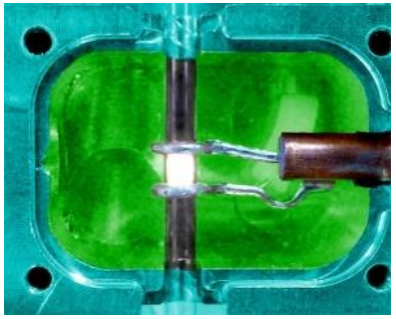

Outline

pd.maguire@ulster.ac.uk

- Some multiple phase examples and applications
- Liquid droplet in plasma
- Droplet charge
- Electron flux to particle

Multiple phase system

pd.maguire@ulster.ac.uk

- The **elements** of the ancients
  - *In no particular order*
  - Earth: Wind: Fire: Water:
- Multiphase systems
  - Combining
  - Multiphase flow
  - Non-equilibrium Plasmas
  - **Solid : Gas : Plasma : Liquid**
- Bringing low temperature plasmas to the Gas-Liquid interface

Solid Gas Plasma Liquid

Multiphase configurations

pd.maguire@ulster.ac.uk

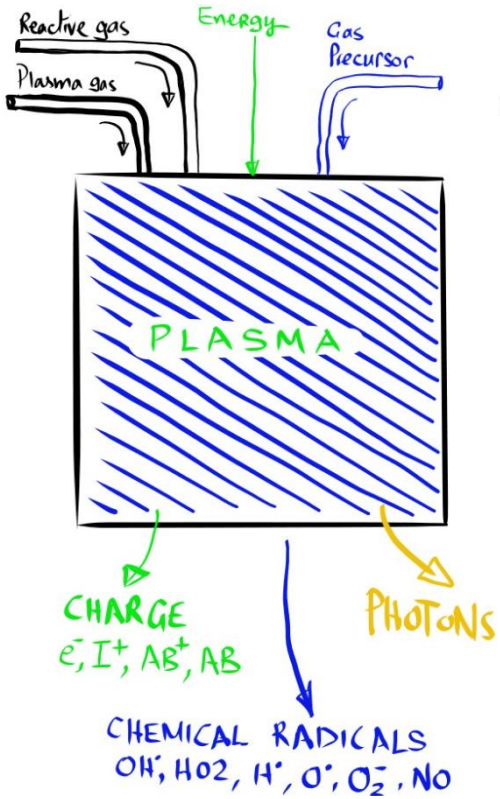

Plasma species & neutral gas molecules, produce energetic charged ions, electrons, photons and radicals

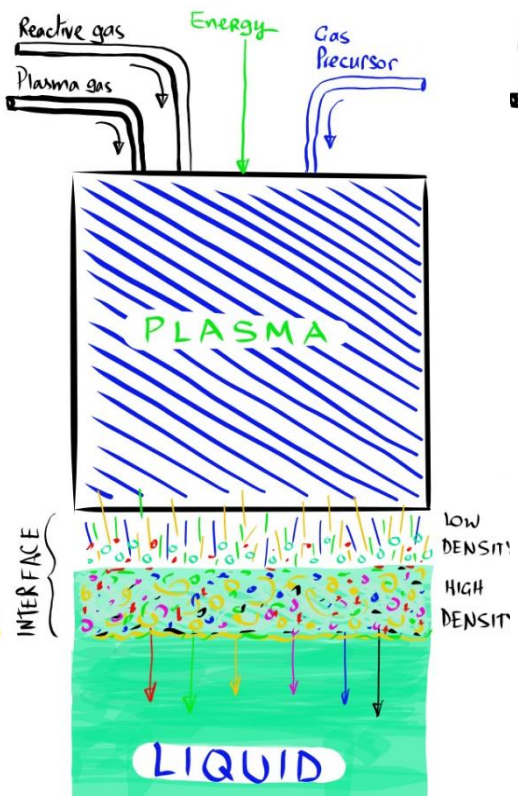

Plasma species & neutral gas molecules, produce energetic charged ions, electrons, photons and radicals.
Transferred to liquid.
Transition region:
- low density layer
- High density layer

Equilibrium region

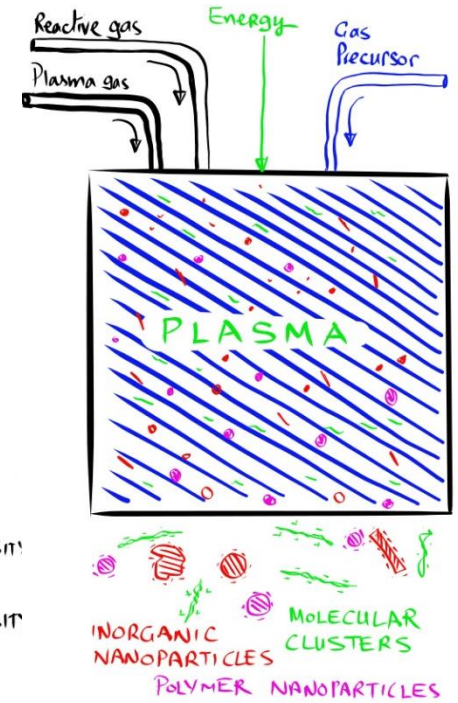

Plasma species & neutral gas molecules, produce energetic charged ions, electrons, photons and radicals.
Gas precursors also create
- molecular clusters
- solid particles

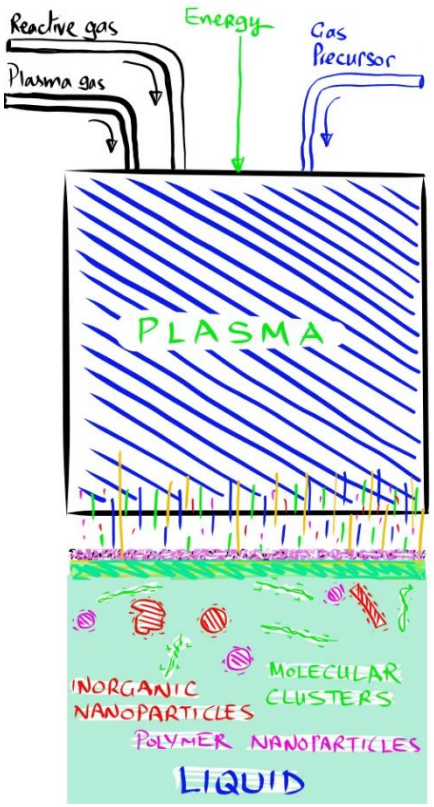

Plasma species & neutral gas molecules, produce energetic charged ions, electrons, photons and radicals.
Transferred to liquid.
Reactions create solid particles

Solid and liquid precursors

pd.maguire@ulster.ac.uk

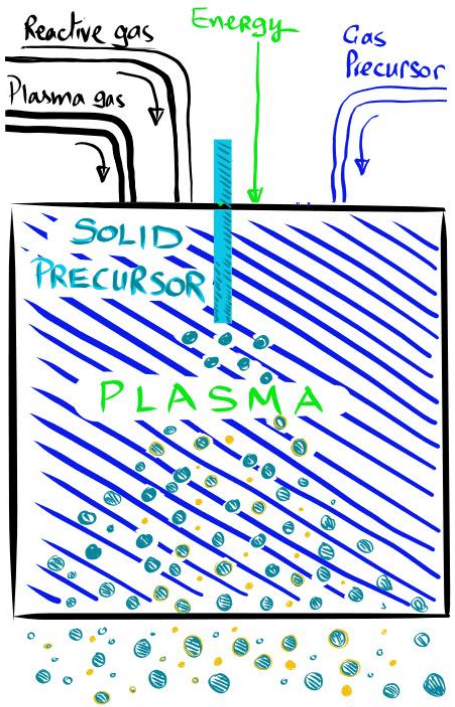

Plasma species & neutral gas molecules, produce energetic charged ions, electrons, photons and radicals.

Solid precursors create
- molecular clusters
- solid particles
- liquid – solid particles

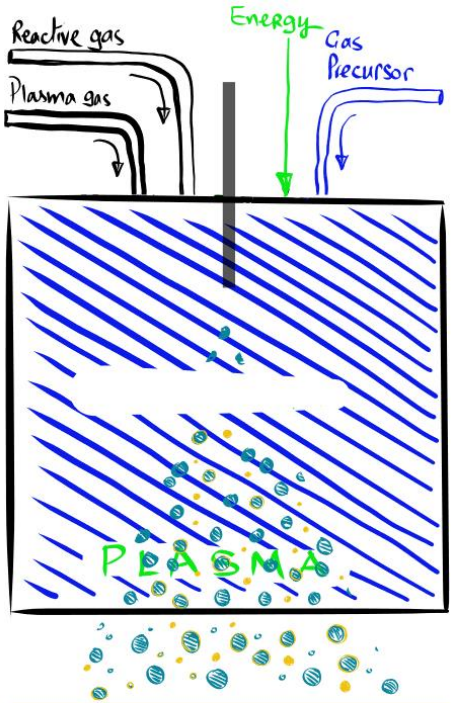

POLYMER
HYDROGEL
POROUS FOAM

Precursors create
- molecular clusters
- solid particles
- liquid – solid particles

Transfer to polymer liquid, hydrogels etc to form nanocomposite

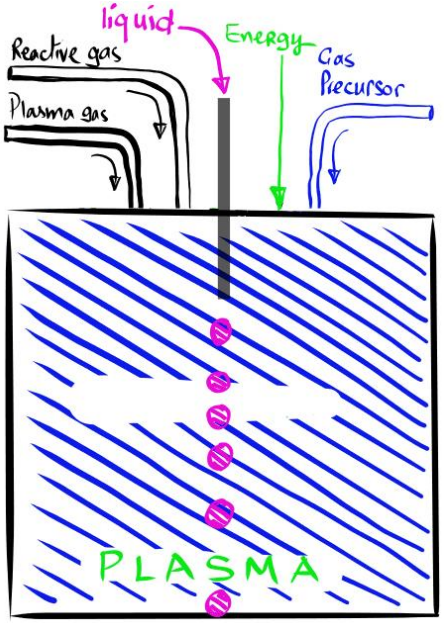

Aerosol Microdroplets

Plasma & neutral gas molecules, produce charged ions, electrons, photons & radicals.

Transferred to liquid drop inside plasma.

Activated droplet

Transported far from plasma

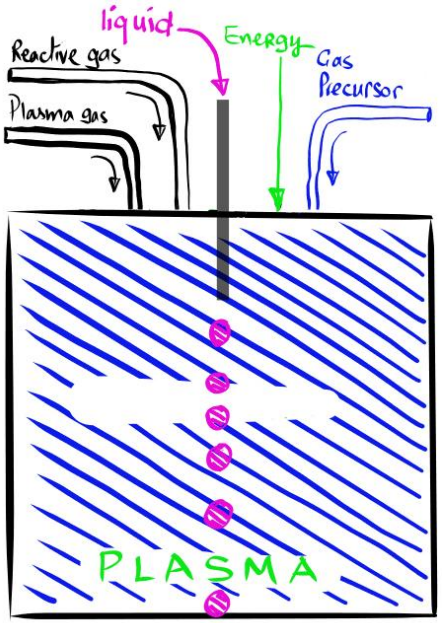

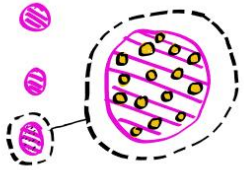

Liquid Microdroplets with solid nanoparticles

Plasma, neutral molecules, produce ions, electrons, photons & radicals.

Transferred to liquid drop with liquid precursor

Nanoparticle synthesis

Transported far from plasma

pd.maguire@ulster.ac.uk

Nanoparticle Synthesis

Plasma charging and heating of particles

Silicon nanoparticles

pd.maguire@ulster.ac.uk

- Plasma interactions
  - SiH_4 monomer dissociation by plasma
  - Molecular assembly → cluster formation
  - Particle assembly
  - Solid surface irradiation by charge & radicals
  - Surface temperature elevation and melting
  - Rapid local annealing and quenching

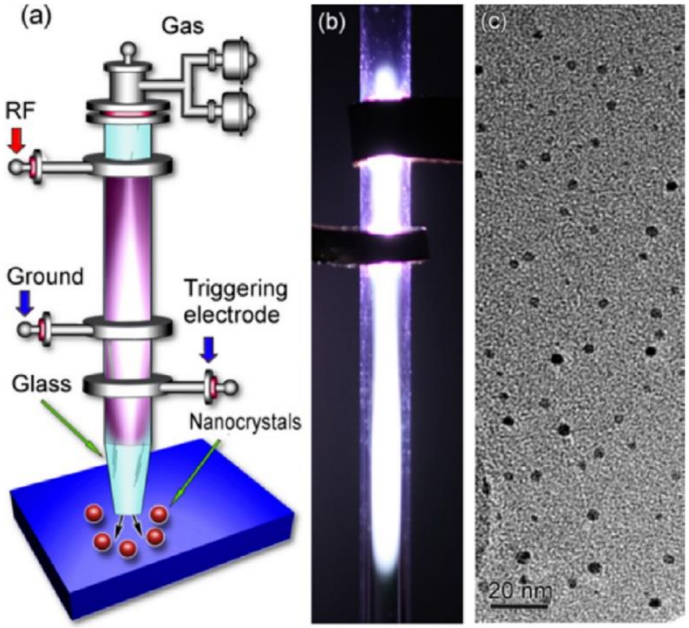

ADVANCED MATERIALS

The Interplay of Quantum Confinement and Hydrogenation in **Amorphous Silicon** Quantum Dots, Askari et al., 2015 10.1002/adma.201503013

Silicon nanoparticles

pd.maguire@ulster.ac.uk

- Plasma interactions
  - SiH_4 monomer dissociation
  - Cluster formation
  - Solid surface irradiation by charge & radicals
  - Surface temperature elevation and melting
  - Rapid local annealing and quenching

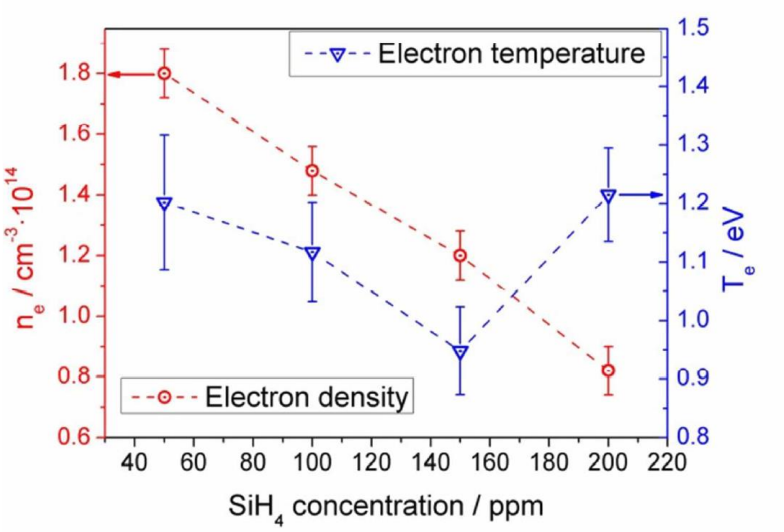

Electron density (left axis) and electron temperature (right axis) calculated

ADVANCED MATERIALS

The Interplay of Quantum Confinement and Hydrogenation in **Amorphous Silicon** Quantum Dots, Askari et al., 2015 10.1002/adma.201503013

Silicon nanoparticles

pd.maguire@ulster.ac.uk

- Plasma interactions
  - SiH_4 monomer dissociation
  - Cluster formation
  - Solid surface irradiation by charge & radicals
  - Surface temperature elevation and melting
  - Rapid local annealing and quenching

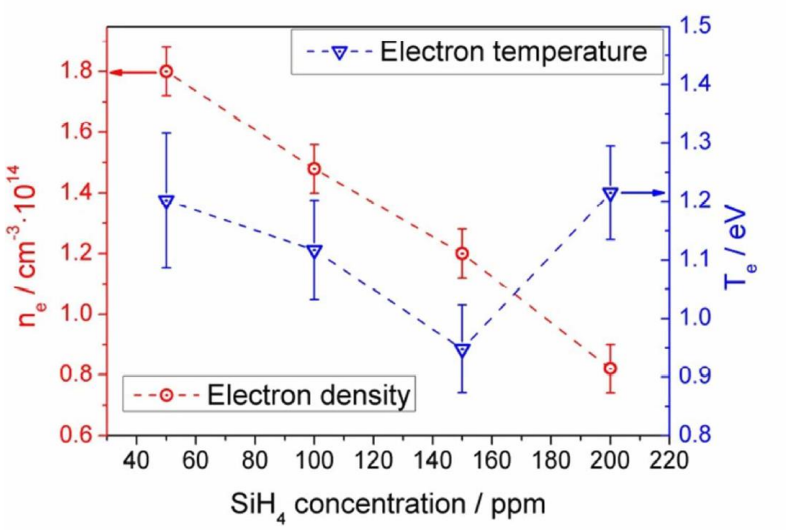

Electron density (left axis) and electron temperature (right axis) calculated

- Hot nanoparticles – Cold gas
  - Tailored semiconductor properties
  - Liquid phase present?
  - Facilitates mass transfer gas → solid ?
- Charge collisional model

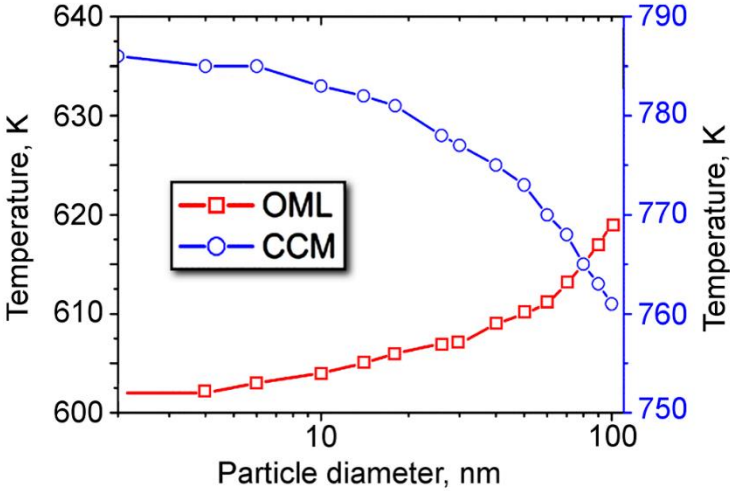

FIG. 4. Particle temperature for a range of nanoparticle diameter according to the two theoretical frameworks, OML, and CCM.

Crystalline Si nanoparticles below crystallization threshold: Effects of collisional heating in non-thermal atmospheric-pressure microplasmas

S. Askari, I. Levchenko, K. Ostrikov, P. Maguire, and D. Mariotti

Citation: Applied Physics Letters **104**, 163103 (2014); doi: 10.1063/1.4872254
View online: http://dx.doi.org/10.1063/1.4872254

ADVANCED MATERIALS

The Interplay of Quantum Confinement and Hydrogenation in **Amorphous Silicon** Quantum Dots, Askari et al., 2015 10.1002/adma.201503013

Silicon nanoparticles

pd.maguire@ulster.ac.uk

- Crystallisation
  - Amorphous – crystalline temperature contour
  - Increase in crystallisation temperature with D
  - Charge flux – size dependent
  - Local surface heating – local melting?
  - Facilitates mass transfer from gas/plasma to solid state

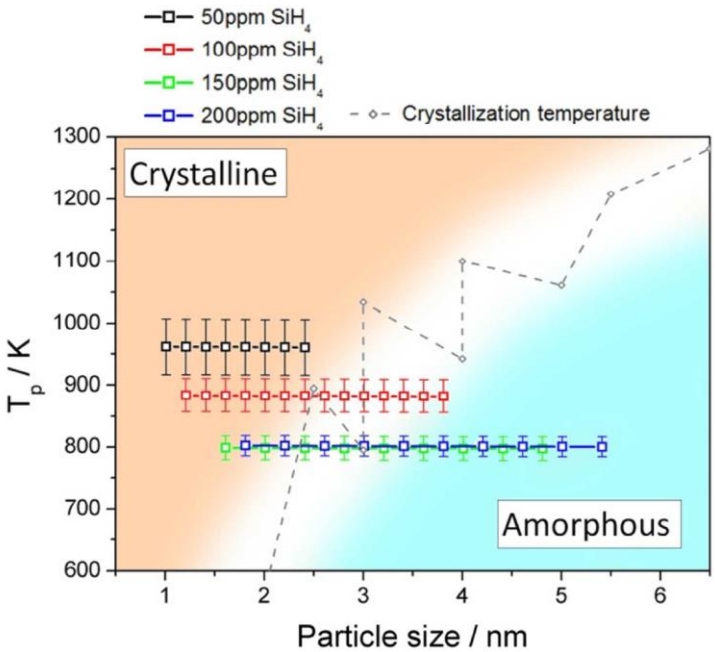

Figure 4. Particle temperature calculated using the collision-corrected model (CCM)

ADVANCED MATERIALS

The Interplay of Quantum Confinement and Hydrogenation in **Amorphous Silicon** Quantum Dots, Askari et al., 2015 10.1002/adma.201503013

Liquid metal, metal clusters

pd.maguire@ulster.ac.uk

- Controlling crystal structure:
  - Ultra-small Sn nanocrystals - from non-equilibrium plasma at atmospheric pressures.
  - Larger nanocrystals adopt the *β*-Sn tetragonal structure,
  - Smaller nanocrystals (< 2nm) show stable *α*-Sn diamond cubic structure.
  - Nanocrystals in the range 2–3 nm, which exhibit mixed phases.
  - Understanding structural stability at the nanoscale
  - Achieving unique phases for different applications.

- Plasma interactions
  - Solid Sn metal precursor
  - Atomic “sputtering” or molten droplet (?)
  - High density microplasma ~10^{20} m^{-3}.
  - Cluster formation or liquid metal droplet
  - Surface irradiation by charge & radicals
  - Surface temperature elevation
  - Rapid local annealing and quenching

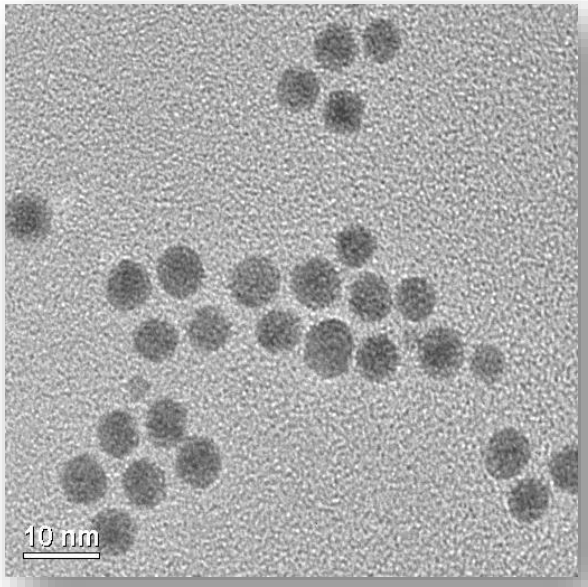

nature COMMUNICATIONS

Haq, A. U. et al Size-dependent stability of ultra-small a-/ß-phase tin nanocrystals synthesized by microplasma. *Nat. Commun.* **2019**, *10* **DOI**:10.1038/s41467-019-08661-9

Droplet In Plasma (DiP)

pd.maguire@ulster.ac.uk

- Plasma - Microdroplets
  - Stream of microdroplets flows through plasma
  - Low gas temperature,
  - “large” size of droplet
  - short residence
  - limited evaporation
  - droplet remains intact

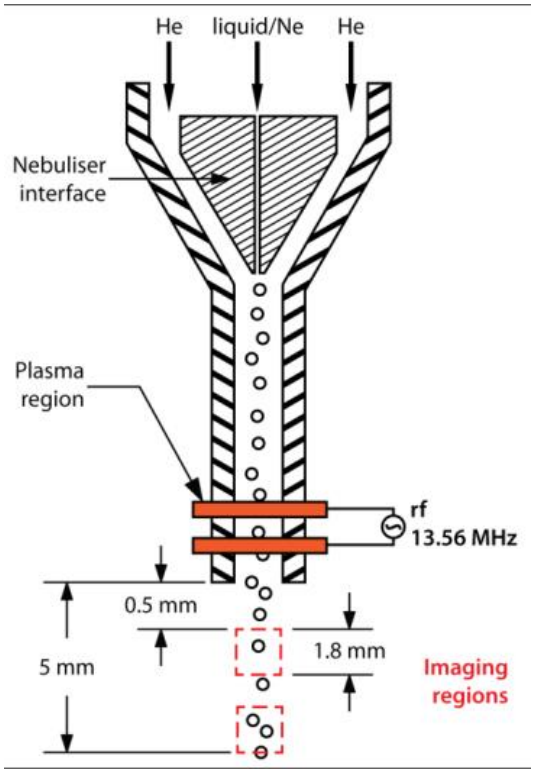

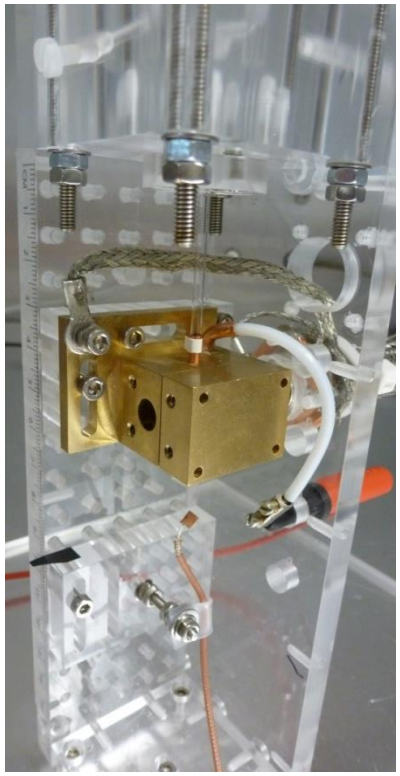

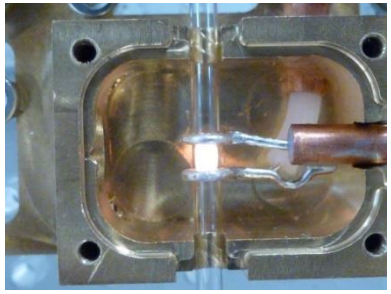

Controlled microdroplet transport in an atmospheric pressure microplasma
P. D. Maguire, C. M. O. Mahony, C. P. Kelsey, A. J. Bingham, E. P. Montgomery, E. D. Bennet, H. E. Potts, D. C. E. Rutherford, D. A. McDowell, D. A. Diver, and D. Mariotti, Appl. Phys. Lett. 106, 224101 (2015), https://doi.org/10.1063/1.4922034

Energy and solar

Biomedical

Plasma - medicine

Optical

Thermal

Applications

Plasma synthesis of nanomaterials

pd.maguire@ulster.ac.uk

- Unique High Value Materials
  - Atmospheric Pressure Plasma Sources
  - Collisional
  - Non-thermal equilibrium
- Multiple Phases
  - Gas-phase synthesis
  - Plasma – cluster
  - Plasma – molten solid - solid
  - Plasma-bulk liquid
  - Plasma-droplet (low evaporation)
  - H2O, ethanol, hydrocarbons, monomers

NANO LETTERS

Continuous In-Flight Synthesis for On-Demand Delivery of Ligand-Free Colloidal Gold Nanoparticles

Paul Maguire*†, David Rutherford†, Manuel Macias-Montero†, Charles Mahony†, Colin Kelsey†, Mark Tweedie†, Fátima Pérez-Martin†, Harold McQuaid†, Declan Diver‡, and Davide Mariotti†

† NIBEC, University of Ulster, Belfast, BT37 0QB, Northern Ireland

‡ SUPA, School of Physics and Astronomy, University of Glasgow, Glasgow G12 8QQ, United Kingdom

Nano Lett., **2017**, *17* (3), pp 1336–1343

DOI: 10.1021/acs.nanolett.6b03440

Cite this: *Nano Lett.* 17, 3, 1336-1343

ADVANCED MATERIALS

Communication | Open Access

The Interplay of Quantum Confinement and Hydrogenation in Amorphous Silicon Quantum Dots

Sadegh Askari, Vladmir Svrcek, Paul Maguire, Davide Mariotti

First published: 02 November 2015 | https://doi.org/10.1002/adma.201503013 | Cited by: 12

NANO LETTERS

Cite This: *Nano Lett.* 2018, 18, 5681−5687

Low-Loss and Tunable Localized Mid-Infrared Plasmons in Nanocrystals of Highly Degenerate InN

Sadegh Askari,*,†,∥ Davide Mariotti,‡ Jan Eric Stehr,† Jan Benedikt,∥ Julien Keraudy,† and Ulf Helmersson†

nature COMMUNICATIONS

Haq, A. U. et al Size-dependent stability of ultra-small a-/ß-phase tin nanocrystals synthesized by microplasma. *Nat. Commun.* **2019**, *10* **DOI**:10.1038/s41467-019-08661-9

PLASMA PROCESSES AND POLYMERS

Feature Article

Plasma–Liquid Interactions at Atmospheric Pressure for Nanomaterials Synthesis and Surface Engineering

Davide Mariotti, Jenish Patel, Vladimir Švrček, Paul Maguire

First published: 06 August 2012 | https://doi.org/10.1002/ppap.201200007 | Cited by: 81

SCIENTIFIC REPORTS

Article | OPEN | Published: 26 October 2015

Enhanced Dispersion of TiO_2 Nanoparticles in a TiO_2/PEDOT:PSS Hybrid Nanocomposite via Plasma-Liquid Interactions

Yazi Liu, Dan Sun, Sadegh Askari, Jenish Patel, Manuel Macias-Montero, Somak Mitra, Richao Zhang, Wen-Feng Lin, Davide Mariotti & Paul Maguire

Scientific Reports **5**, Article number: 15765 (2015) | Download Citation

nature COMMUNICATIONS

Article | OPEN | Published: 01 August 2017

Charge carrier localised in zero-dimensional $(CH_3NH_3)_3Bi_2I_9$ clusters

Chengsheng Ni, Gordon Hedley, Julia Payne, Vladimir Svrcek, Calum McDonald, Lethy Krishnan Jagadamma, Paul Edwards, Robert Martin, Gunisha Jain, Darragh Carolan, Davide Mariotti, Paul Maguire, Ifor Samuel & John Irvine

Green Chemistry — ROYAL SOCIETY OF CHEMISTRY

PAPER — View Article Online

Check for updates

Cite this: DOI: 10.1039/d0gc03291c

Understanding plasma–ethanol non-equilibrium electrochemistry during the synthesis of metal oxide quantum dots†

Dilli Babu Padmanaban,*a Ruairi McGlynn,a Emily Byrne,b Tamilselvan Velusamy,a Małgorzata Swadźba-Kwaśny,b Paul Maguire,a and Davide Mariotti*a

ACS APPLIED MATERIALS & INTERFACES

Microplasma Processed Ultrathin Boron Nitride Nanosheets for Polymer Nanocomposites with Enhanced Thermal Transport Performance

Ri-Chao Zhang*†‡§, Dan Sun*†, Ai Lu‡, Sadegh Askari∥, Manuel Macias-Montero§, Paul Joseph‡, Dorian Dixon§, Kostya Ostrikov†▲, Paul Maguire§, and Davide Mariotti§

† Department of Chemical and Biological Engineering, Zhejiang University, Hangzhou, 310002, PR China

‡ School of Mechanical and Aerospace Engineering, Queen's University Belfast, BT9 5AH, U.K.

§ Nanotechnology and Integrated Bioengineering Centre (NIBEC), University of Ulster, Newtownabbey, BT37 0QB, Northern Ireland, U.K.

ELSEVIER — Nano Energy

Volume 50, August 2018, Pages 245-255

https://doi.org/10.1016/j.nanoen.2018.05.036

Full paper

Type-I alignment in $MAPbI_3$ based solar devices with doped-silicon nanocrystals

Conor Rocks[a], Vladimir Svrcek[b], Tamilselvan Velusamy[a], Manuel Macias-Montero[a], Paul Maguire[a], Davide Mariotti[a]

Green Chemistry

Microplasma-assisted electrochemical synthesis of Co_3O_4 nanoparticles in absolute ethanol for energy applications

Chengsheng Ni,*[abc] Darragh Carolan,[a] Conor Rocks,[a] Jianing Hui,[b] Zeguo Fang,[b] Dilli Babu Padmanaban,[a] Jiupai Ni,[c] Deti Xie,[c] Paul Maguire,[a] John T. S. Irvine[b] and Davide Mariotti[a]

ROYAL SOCIETY OF CHEMISTRY

DOI: 10.1039/C7SE00158D (Paper) *Sustainable Energy Fuels*, 2017, 1, 1611-1619

Environmentally friendly nitrogen-doped carbon quantum dots for next generation solar cells†

Darragh Carolan*[a], Conor Rocks[a], Dilli Babu Padmanaban[a], Paul Maguire[a], Vladimir Svrcek[a] and Davide Mariotti[a]

[a]Nanotechnology & Integrated Bio-Engineering Centre (NIBEC), Ulster University, Jordanstown, Newtownabbey, Co. Antrim BT37 0QB, UK. E-mail: d.carolan@ulster.ac.uk

[b]Research Centre of Photovoltaics, National Institute of Advanced Industrial Science and Technology-AIST, Central 2, Tsukuba, Japan

Plasma induced chemical reduction in droplets

pd.maguire@ulster.ac.uk

- Solids formed in liquids in gas/plasma

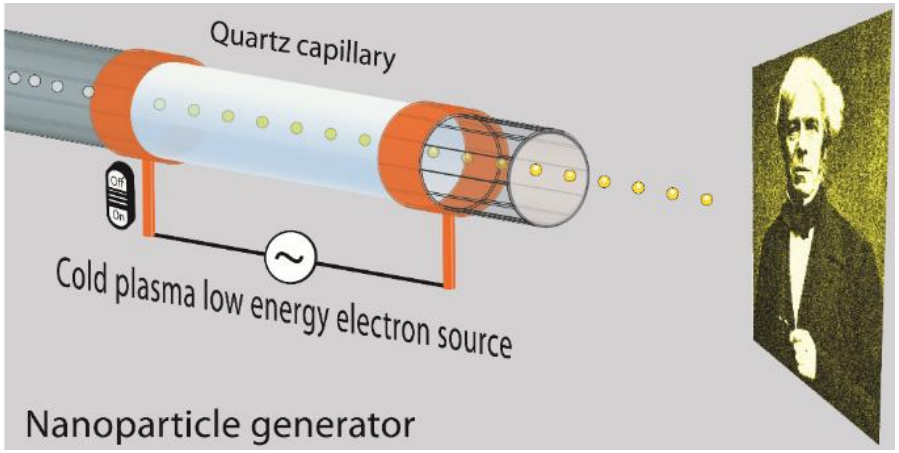

- Nanoparticles: on demand delivery
  - ➲$HAuCl_4$ in H_2O microdroplet
  - ➲Passed through plasma
  - ➲120 us time of flight
- Electron flux
  - ➲Direct reduction of Au^{3+} ions in liquid by solvated electrons from plasma

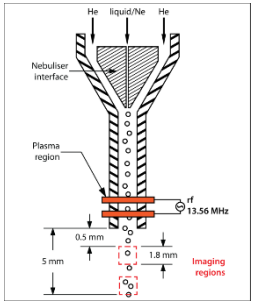

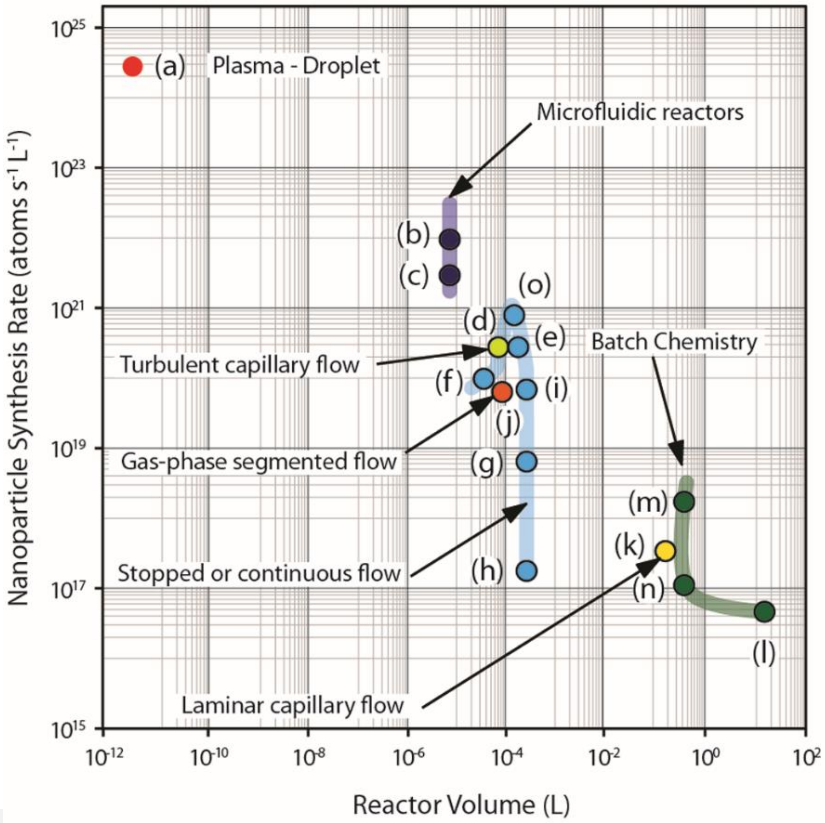

Comparison of plasma – droplet synthesis rate with batch and microreaction chemistry

NANO LETTERS

Continuous In-Flight Synthesis for On-Demand Delivery of Ligand-Free Colloidal Gold Nanoparticles, Maguire et al., Nano Letts., 2017, https://dx.doi.org/10.1021/acs.nanolett.6b03440

Plasma versus Radiolysis or e-Beam

pd.maguire@ulster.ac.uk

- X 10^3 – 10^7 faster
  - **Similar dose rate as gamma radiation**
- Plasma-droplet
  - Dose rate assuming **x%** plasma energy delivered to drop
  - 5×10^{-2} kGy s^{-1}.

$HAuCl_4$. The reduction of **Au^{III}** proceeds via reactions as:

II	$Au^{III}Cl_4^- + e_{aq}^- \rightarrow Au^{II}Cl_4^{2-}$	(R1)
III / I	$2\ Au^{II}Cl_4^{2-} \rightarrow Au^{III}Cl_4^- + Au^{I}Cl_2^- + 2Cl^-$	(R2a)
0	$\mathbf{Au^{I}Cl_2^- + e_{aq}^- \rightarrow Au^{0}Cl_2^{2-}}$	**(R3)**
I / II	$Au^{III} + Au^0 \rightarrow Au^{I}$ and Au^{II}	(R4)

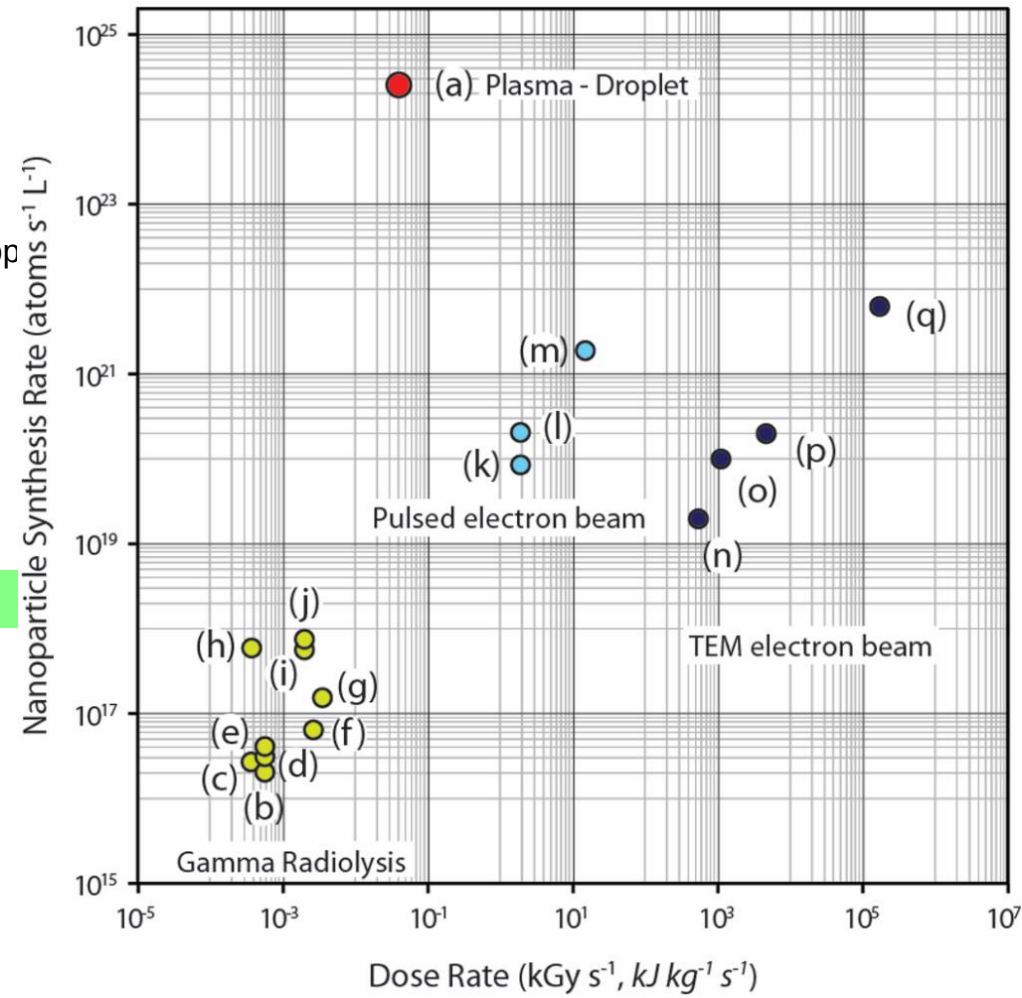

Comparison of plasma – droplet synthesis rate with high energy radiolysis or electron beam methods

Continuous In-Flight Synthesis for On-Demand Delivery of Ligand-Free Colloidal Gold Nanoparticles, Maguire et al., Nano Letts., 2017, https://dx.doi.org/10.1021/acs.nanolett.6b03440

Microdroplet delivery of OH

pd.maguire@ulster.ac.uk

- Methylene Blue indicator destruction
- Significant increase in OH delivered using microdroplets

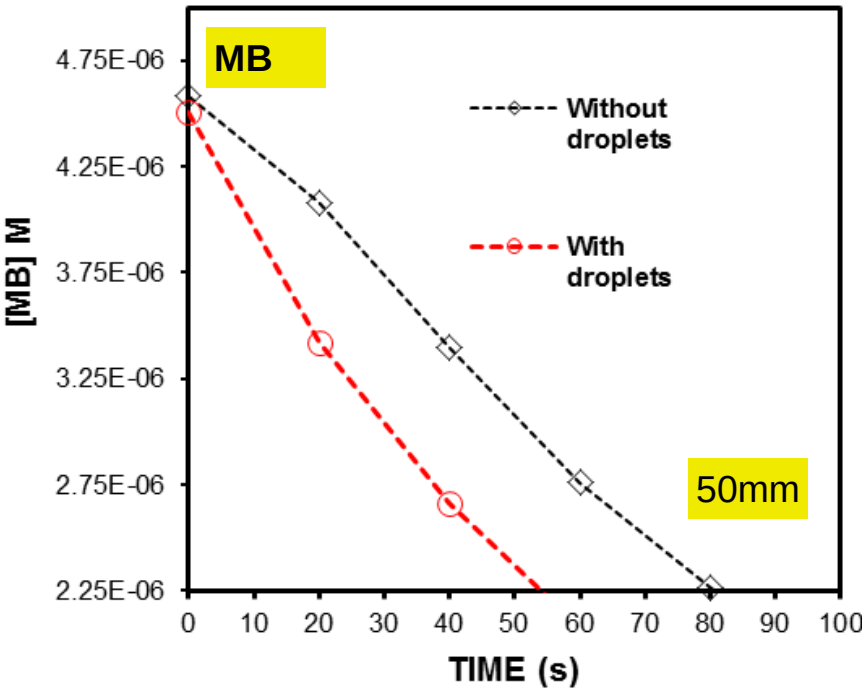

Droplet OH delivery and E coli destruction

pd.maguire@ulster.ac.uk

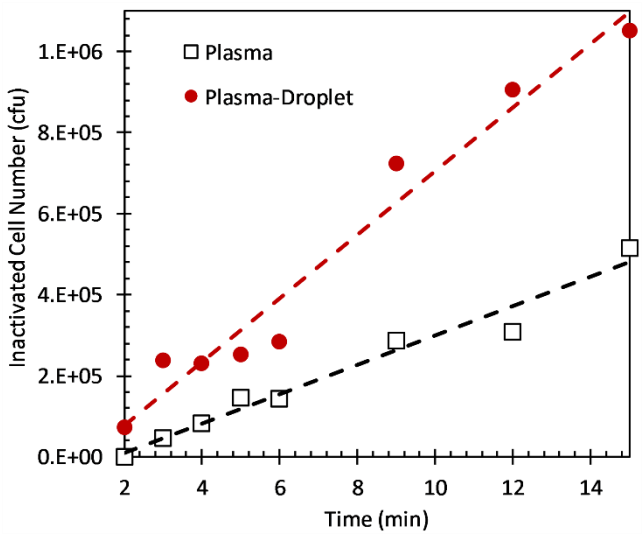

No of cells inactivated versus PE and PED exposure time at a fixed distance of 4.3 cm, calculated from ZoI diameter assuming ~4000 cfu mm^{-2}.

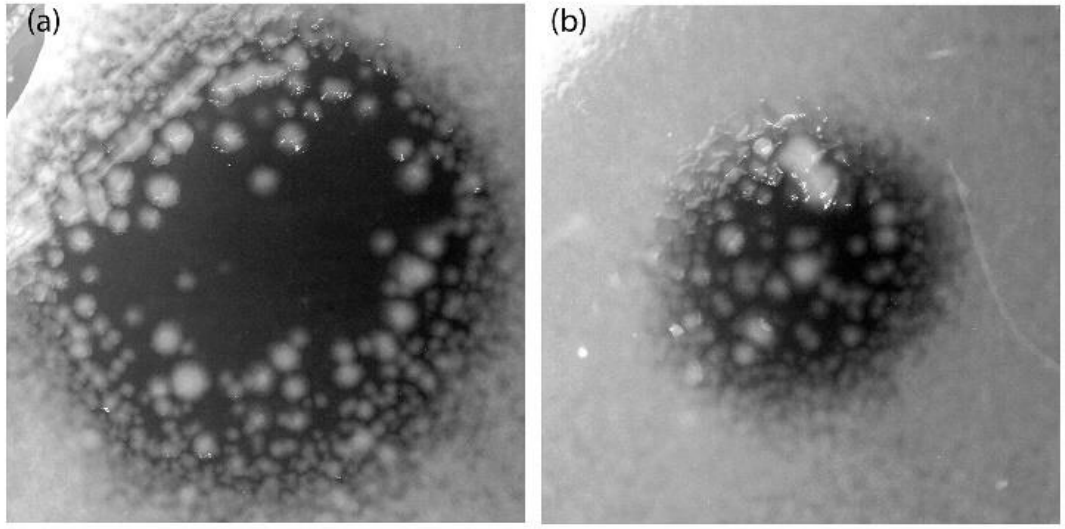

E coli growth inhibition zone (ZoI) at a distance of 40 mm from plasma, after 3 min exposure to
(a) plasma effluent with **droplets** and
(b) plasma effluent

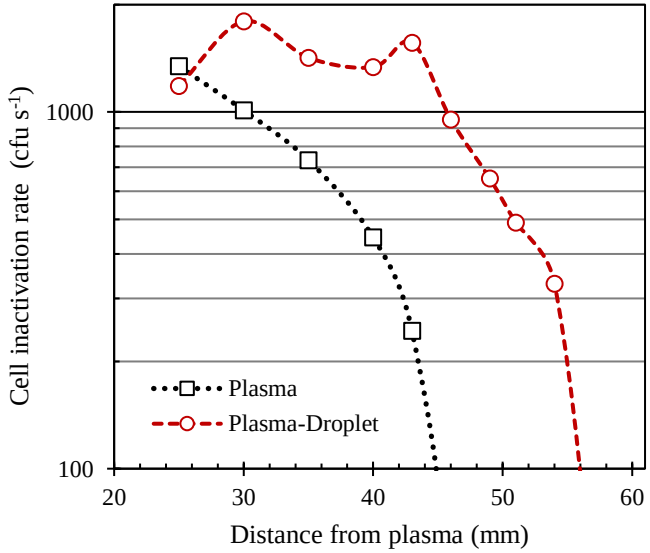

Increased efficacy in killing E coli with distance using droplets

Cell inactivation rate versus distance

pd.maguire@ulster.ac.uk

- Cell inactivation rate vs distance from plasma
- Plasma only (black)
  - RF plasma
  - Plasma – free effluent a few millimetres beyond electrode
  - No ionization waves / bullets
  - Inactivation efficacy determined by reach of effluent
- Plasma + Droplets (red)
  - Open air delivery
  - Efficacy extends to larger distances
  - Extra is due to droplet reactivity
- Plasma + Droplets in a flexible tube (blue)
  - Shielded delivery
  - Droplets shielded from turbulence at plasma exit
  - Inactivation efficacy extends further
  - Extra is due to droplet reactivity
  - Possible limits of reactive species lifetime
- Plasma exposed droplets: increased efficacy in killing E coli over larger distances

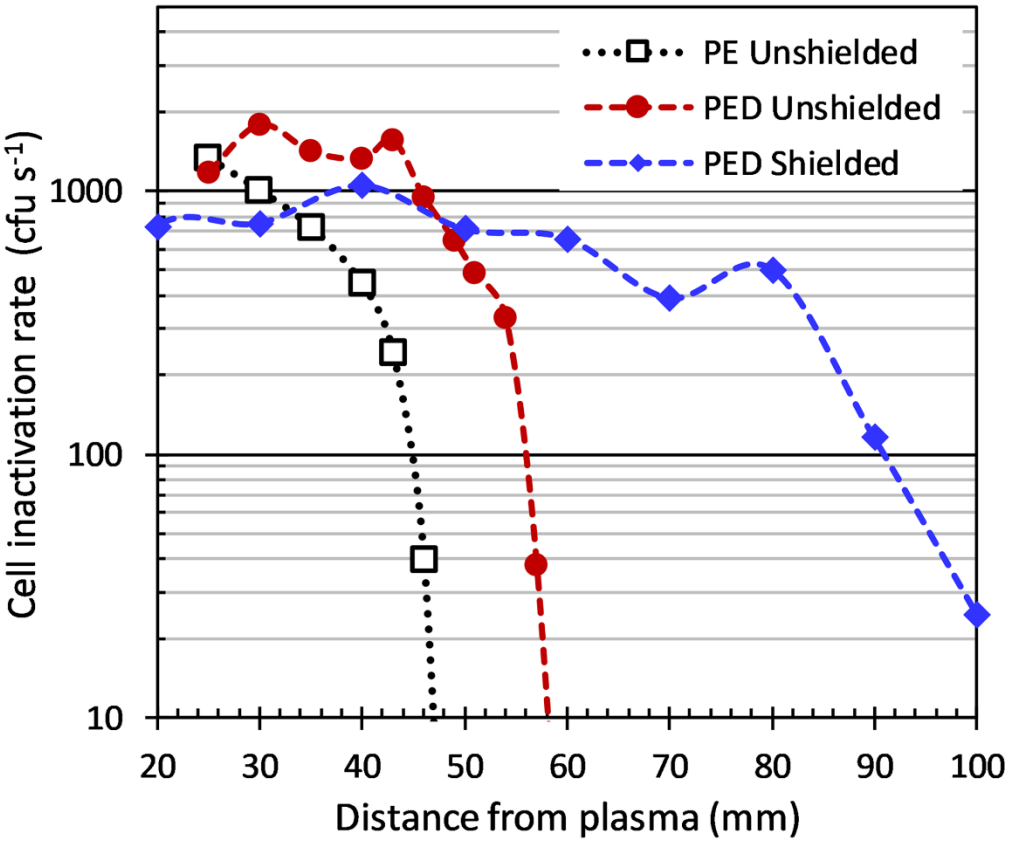

Droplets - cancer

pd.maguire@ulster.ac.uk

- Tumour cells
  - In-vitro
  - Colorectal tumour cells: HT29, CaC0-2
  - 3 min exposure to droplets, fixed distance
  - 24h culture

- Cell viability
  - Significant reduction in cell viability after short exposure due to reactive droplets

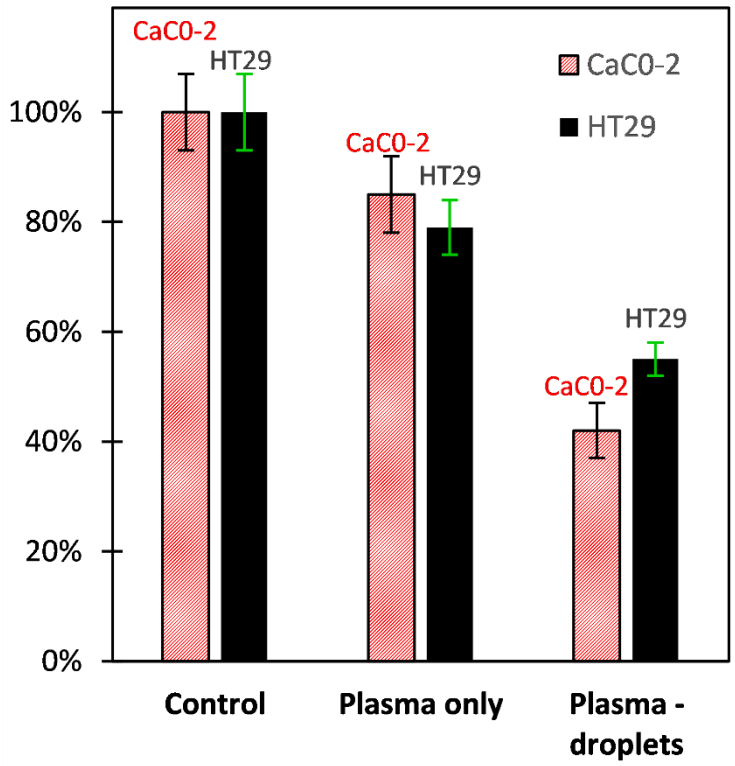

Microdroplets containing L-Cysteine amino acid

pd.maguire@ulster.ac.uk

- L-Cysteine loaded microdroplets
  - Limit of detection
  - 100 mM (x 100 higher)
  - 250 us plasma exposure
  - 99.5% conversion
  - IPA scavenging prevents most of conversion

Plasma – liquid reaction rate = 3 x 10^{-6} M s^{-1}

Plasma – droplet reaction rate = 400 M s^{-1}

8 orders of magnitude increase

L-Cysteine loaded (100 mM) microdroplets

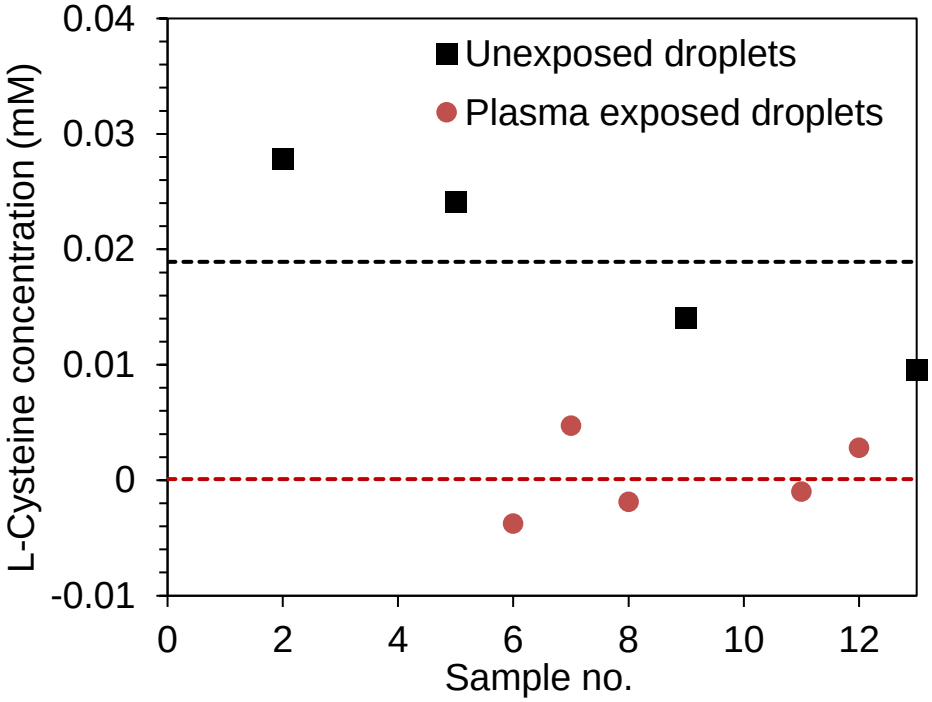

L-Cysteine with IPA

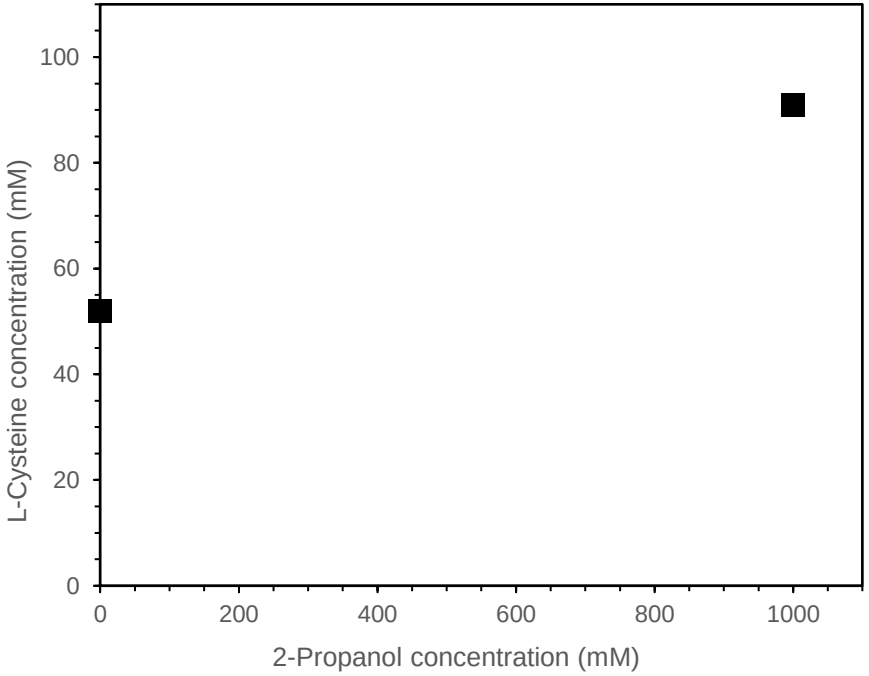

E coli cell in droplet

pd.maguire@ulster.ac.uk

- Plasma-induced lipid peroxidation
  - Significant MDA level obtained for plasma CT
  - Equivalent MDA level obtained from H_2O_2 at 10^4 x CT of droplet H_2O_2.
  - **Evidence for direct OH interaction**
- Literature – plasma
  - Dolezalova, Alkawareek, Kim, Lee
  - MDA (uM levels) in minutes - hours

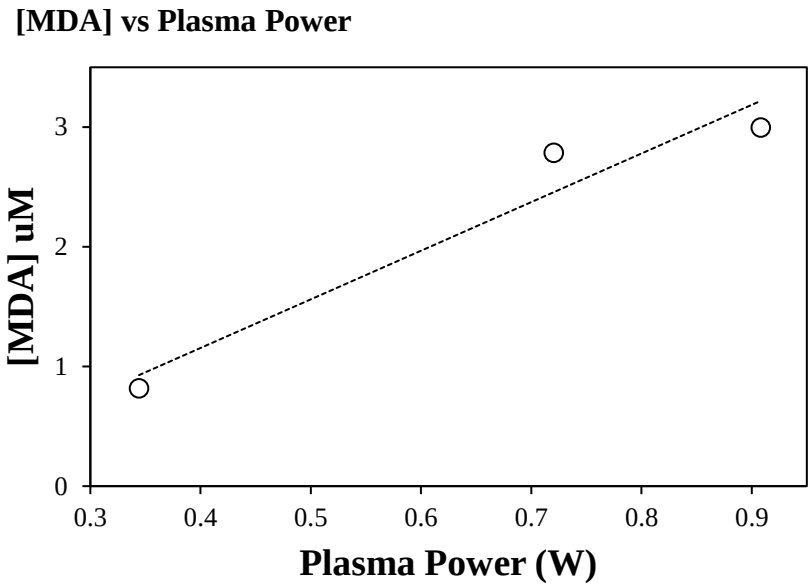

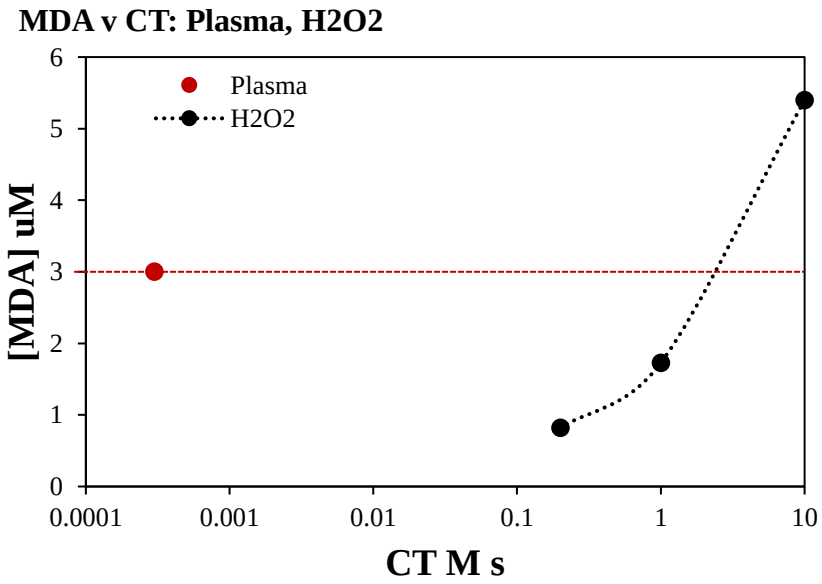

Droplet in Plasma (DiP)

Droplet In Plasma (DiP)

pd.maguire@ulster.ac.uk

- Microscale droplets
  - A stream of microdroplets transported through a low temperature RF plasma.
  - Low gas temperature, “large” size of droplet and short residence means evaporation is incomplete
- Non-thermal equilibrium plasma
  - Gas, ion temperature << electron temperature
  - $T_{gas} \sim T_{ion} << T_e$.
- Plasma - Microdroplets
  - Stream of microdroplets flows through plasma
  - 50,000 droplets / sec
  - Exposed to plasma for **~120 μs**
  - Droplet mean velocity **~10 ms^{-1}**

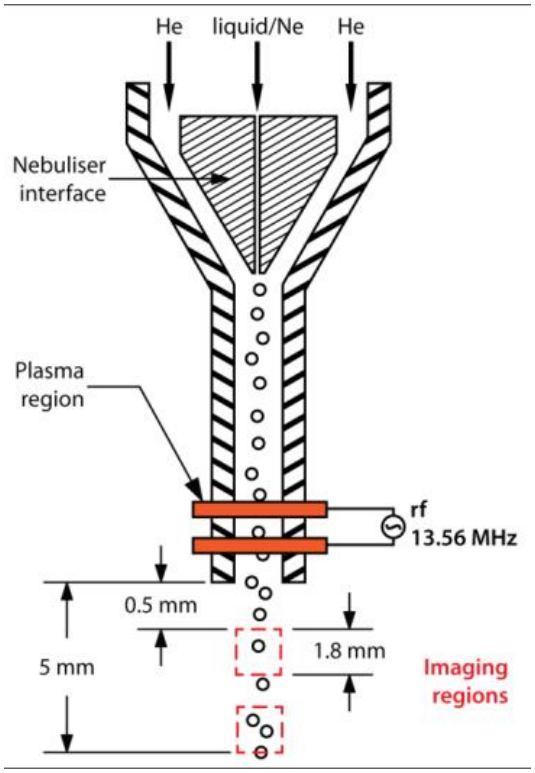

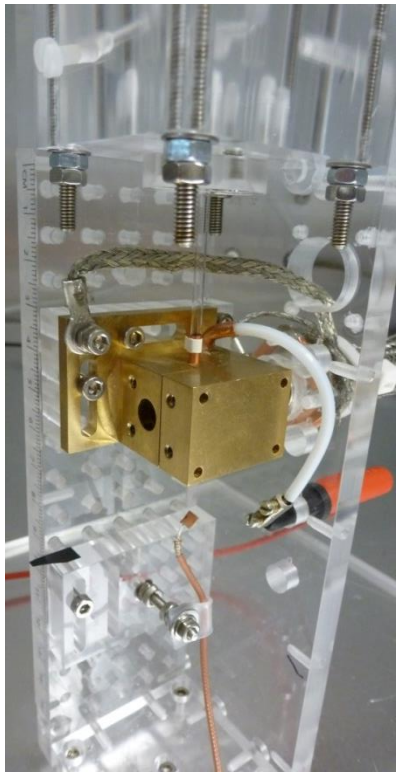

RF 13.56 MHz,
He: 3.5 slm,
Ne (aerosol): 1 slm
or Ar (aerosol): 1 slm

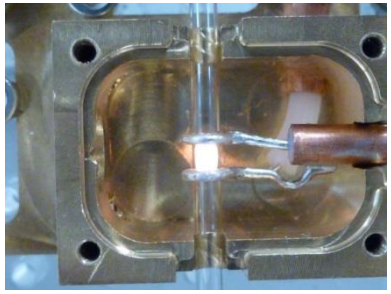

Maguire et al., Appl. Phys. Lett. 106, 224101 (2015);

Plasma chemistry, into liquid

pd.maguire@ulster.ac.uk

- Without droplets
- Humidity
  - Net input power decreases > 500ppm, as plasma becomes electronegative
  - Power density (emission brightness) decreases at slower rate

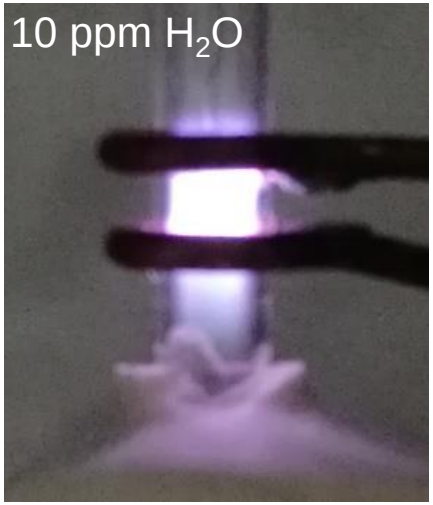

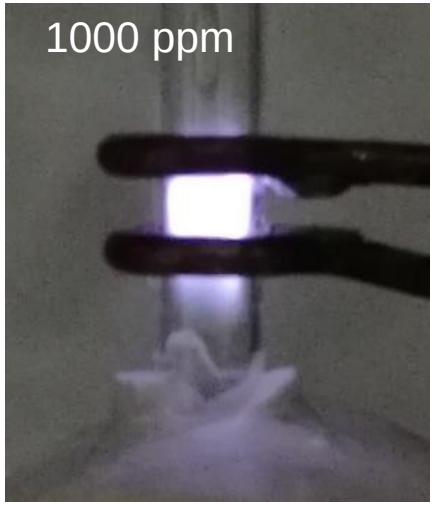

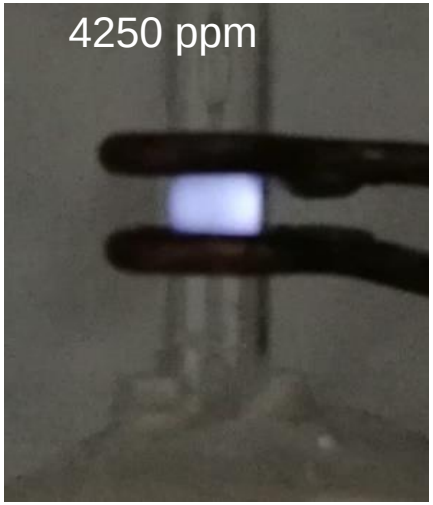

Plasma chemistry, into liquid

pd.maguire@ulster.ac.uk

- Without droplets
- Humidity
  - Net input power decreases > 500ppm, as plasma becomes electronegative
  - Power density (emission brightness) decreases at slower rate
- OH maximum
  - Peaks ~500 ppm

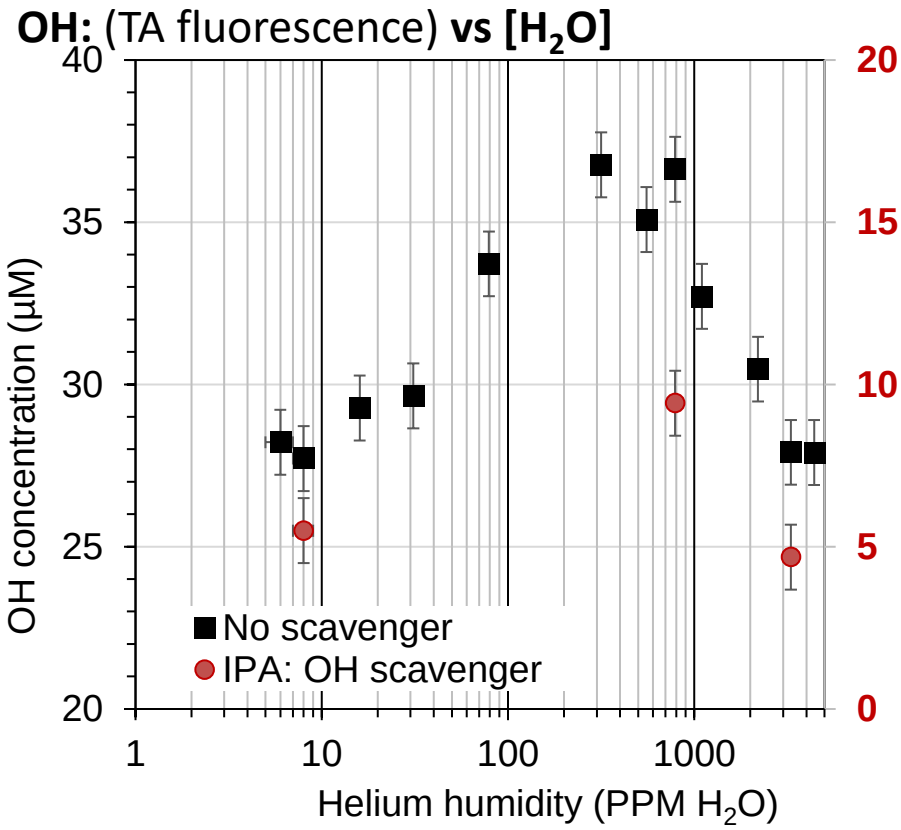

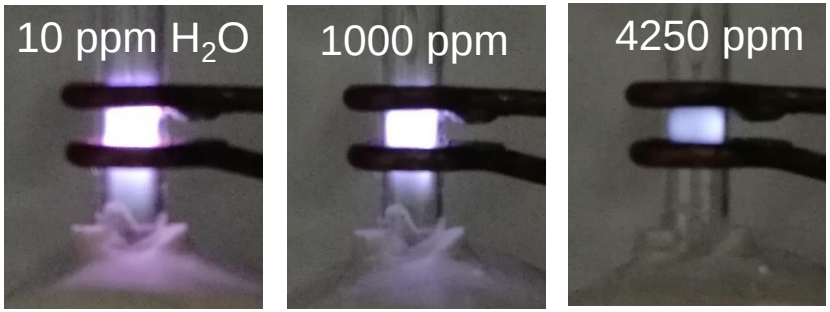

Plasma chemistry, into liquid

pd.maguire@ulster.ac.uk

- Without droplets
- Humidity
  - ➲Net input power decreases > 500ppm, as plasma becomes electronegative
  - ➲Power density (emission brightness) decreases at slower rate
- OH maximum
  - ➲ Peaks ~500 ppm
  - ➲ Reduction in power density > 500 ppm

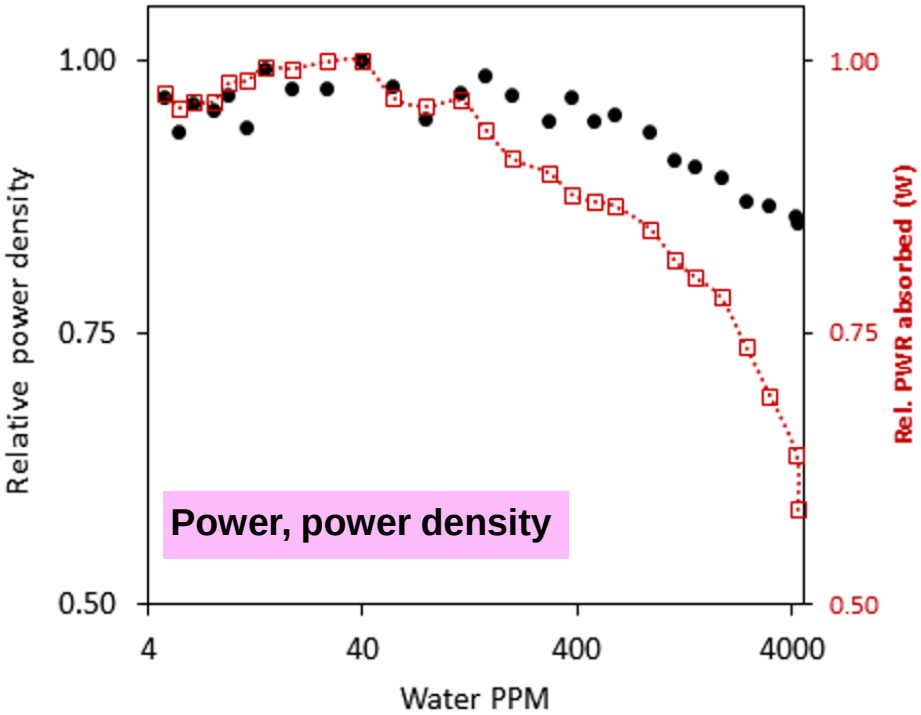

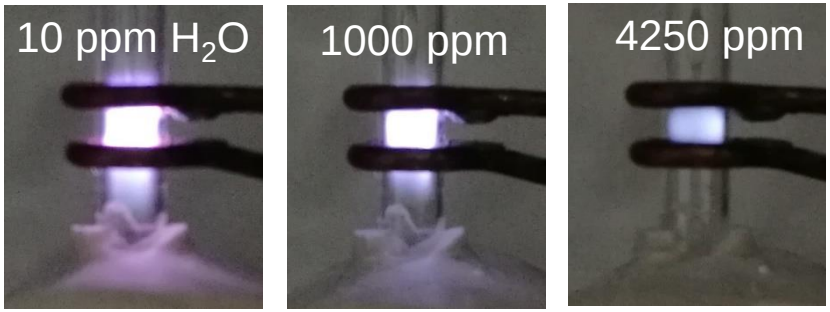

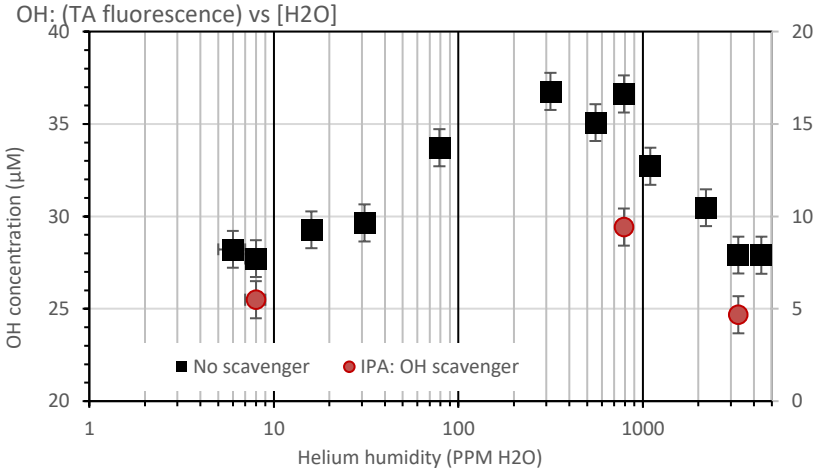

Gas temperature

pd.maguire@ulster.ac.uk

- IR temperature measurement
  - Focal spot: minimum < 0.6 mm
  - Calibrated – inner wall of plasma capillary tube
  - Temperature readings – outer wall.

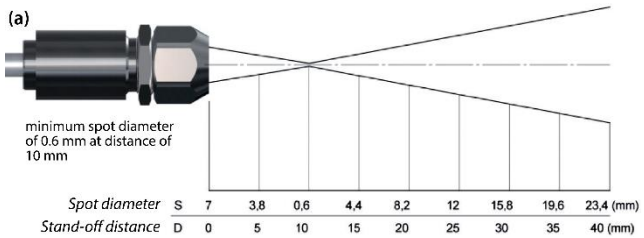

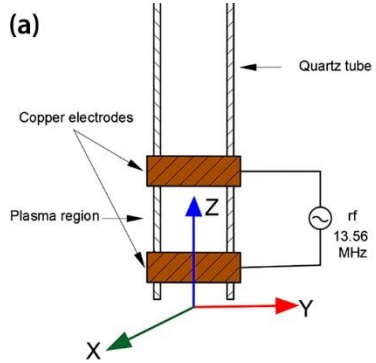

Plasma: electrodes and capillary

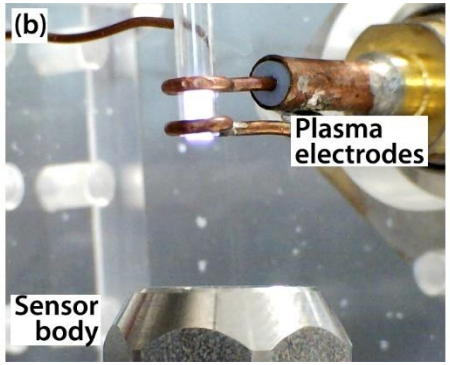

Calibration mode
Vertical – inner wall

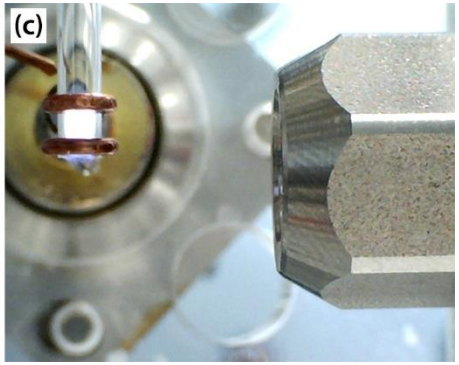

Measurement mode
Horizontal – outer wall

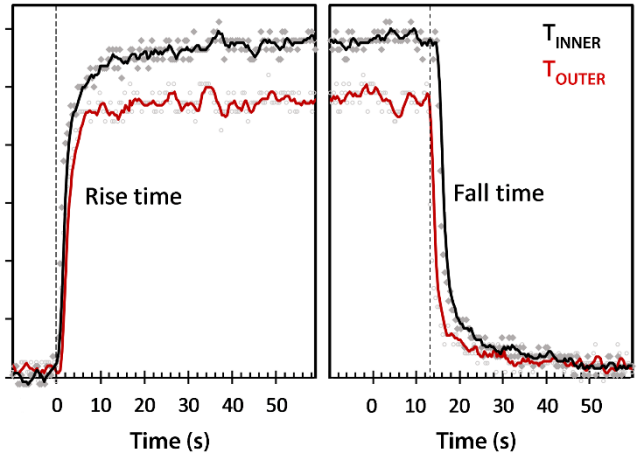

Temperature rise and fall times for inner wall (black) and outer wall (red). Dashed lines indicate the plasma ignition and extinction times obtained from photodiode response.

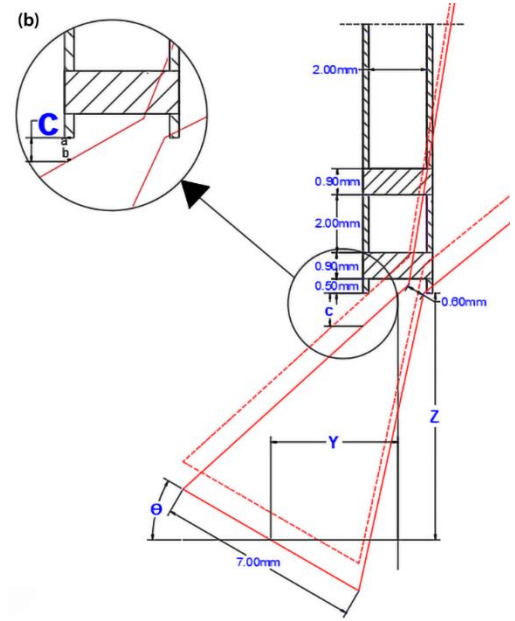

Calibration mode
Vertical – inner wall

Continuous gas temperature measurement of cold plasma jets containing microdroplets, using a focussed spot IR sensor
N Hendawy *et al* 2020 *Plasma Sources Sci. Technol.* **29** 085010
https://doi.org/10.1088/1361-6595/aba2aa

Gas temperature

pd.maguire@ulster.ac.uk

- Plasma only
  - Range: 28 °C to 45 °C
  - Depends on power, flow

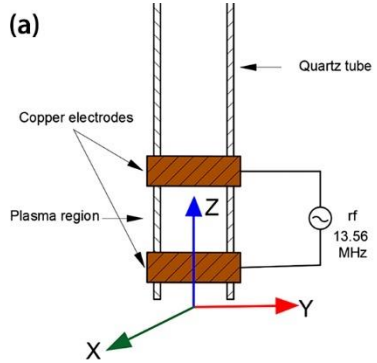

Plasma: electrodes and capillary

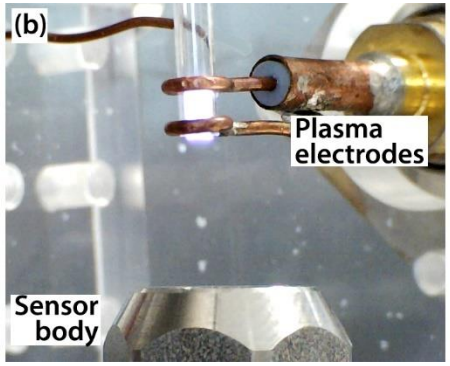

Calibration mode
Vertical – inner wall

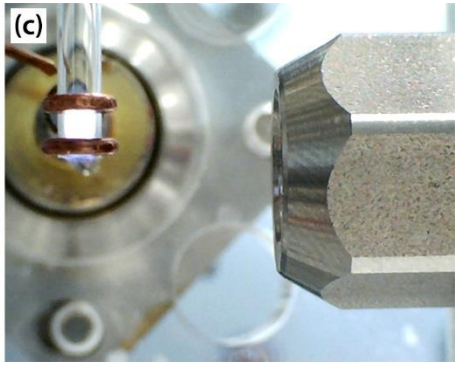

Measurement mode
Horizontal – outer wall

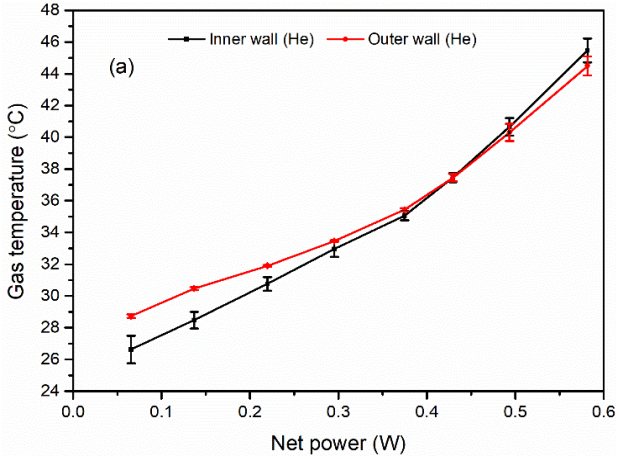

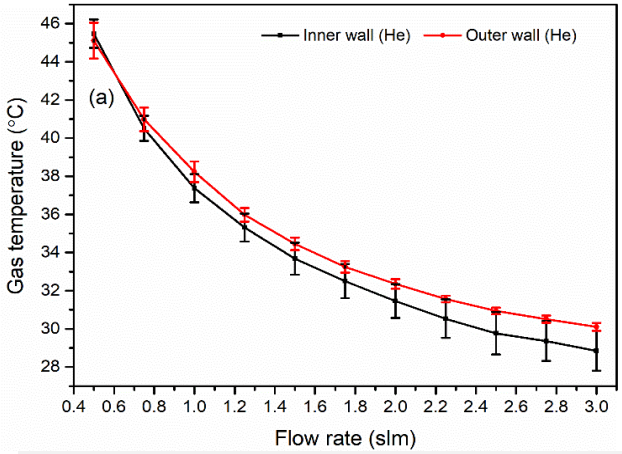

Continuous gas temperature measurement of cold plasma jets containing microdroplets, using a focussed spot IR sensor
N Hendawy *et al* 2020 *Plasma Sources Sci. Technol.* **29** 085010
https://doi.org/10.1088/1361-6595/aba2aa

Gas temperature

pd.maguire@ulster.ac.uk

- Plasma with droplets
  - Reduction in temperature, up to 12 ^{o}C.
  - Depends on power, flow

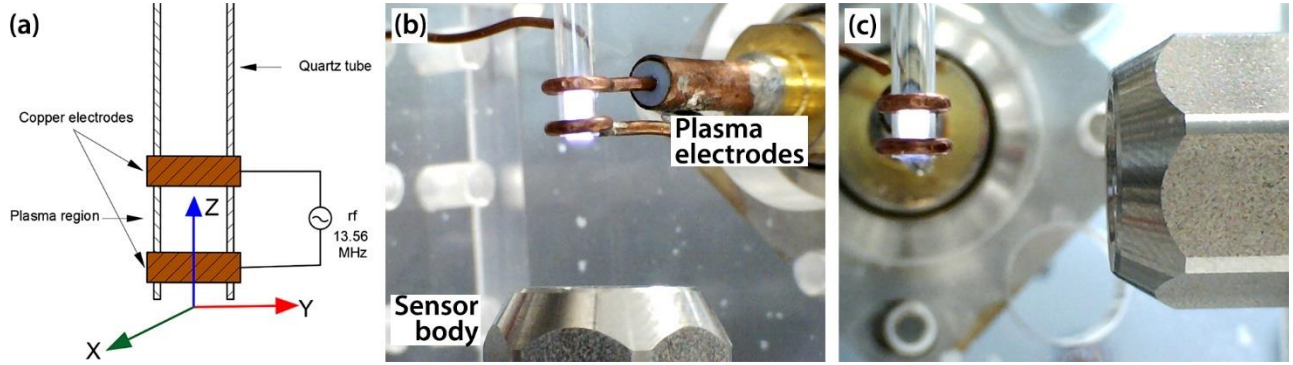

Plasma: electrodes and capillary | Calibration mode Vertical – inner wall | Measurement mode Horizontal – outer wall

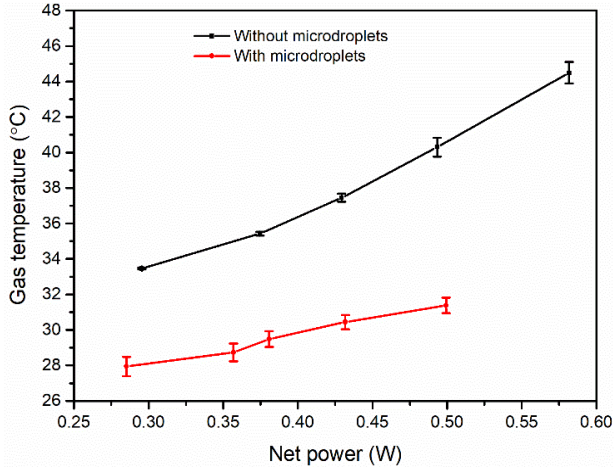

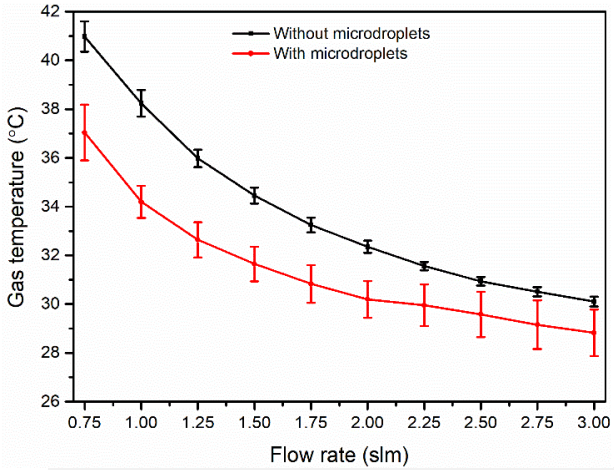

Continuous gas temperature measurement of cold plasma jets containing microdroplets, using a focussed spot IR sensor
N Hendawy *et al* 2020 *Plasma Sources Sci. Technol.* **29** 085010
https://doi.org/10.1088/1361-6595/aba2aa

Temperature Comparison

pd.maguire@ulster.ac.uk

RF Plasma jets, different configurations

- Sremački 2021: ~300 K, no increase with droplets
  - Estimate, no measurement

Influence of aerosol injection on the liquid chemistry induced by an RF argon plasma jet
Ivana Sremački, Giuliana Bruno, Helena Jablonowski, Christophe Leys, Anton Yu Nikiforov and Kristian Wende, (2021) Plasma Sources Sci. Technol. *In press.* https://doi.org/10.1088/1361-6595/abe176

- Oinuma 2020: 320 K – 350 K
  - OH(*A*) emission
  - Measured: plasma only, no droplets
  - Temperature increases in direction of flow

Controlled plasma–droplet interactions: a quantitative study of OH transfer in plasma–liquid interaction
Gaku Oinuma, Gaurav Nayak, Yanjun Du and Peter J Bruggeman, 2020 *Plasma Sources Sci. Technol.* **29** 095002, https://doi.org/10.1088/1361-6595/aba988

- Nitta 2021: 1000 K – 1100 K
  - N_2 2nd positive system
  - Measured: plasma with droplets

Plasma-assisted synthesis of size-controlled monodisperse submicron gold particles using inkjet droplets
Kaishu Nitta, Yoshiki Shimizu, Kazuo Terashima and Tsuyohito Ito, 2021 *J. Phys. D: Appl. Phys.* **54** 33LT01, https://doi.org/10.1088/1361-6463/ac02f8

Basic plasma, droplet conditions

Basic plasma – droplet conditions

pd.maguire@ulster.ac.uk

RF 13.56MHz
n_e: 10^{12} – 10^{14} cm^{-3}.
Reactor diameter: 2mm

HeNe plasma (5:1)
Laminar axial flow
~10^4 droplets per second
Residence time in plasma: ~100μs
Droplet diameter average: 15 μm

He^0 neutrals
He^*
Ne^0

He^+ ions
Ne^+

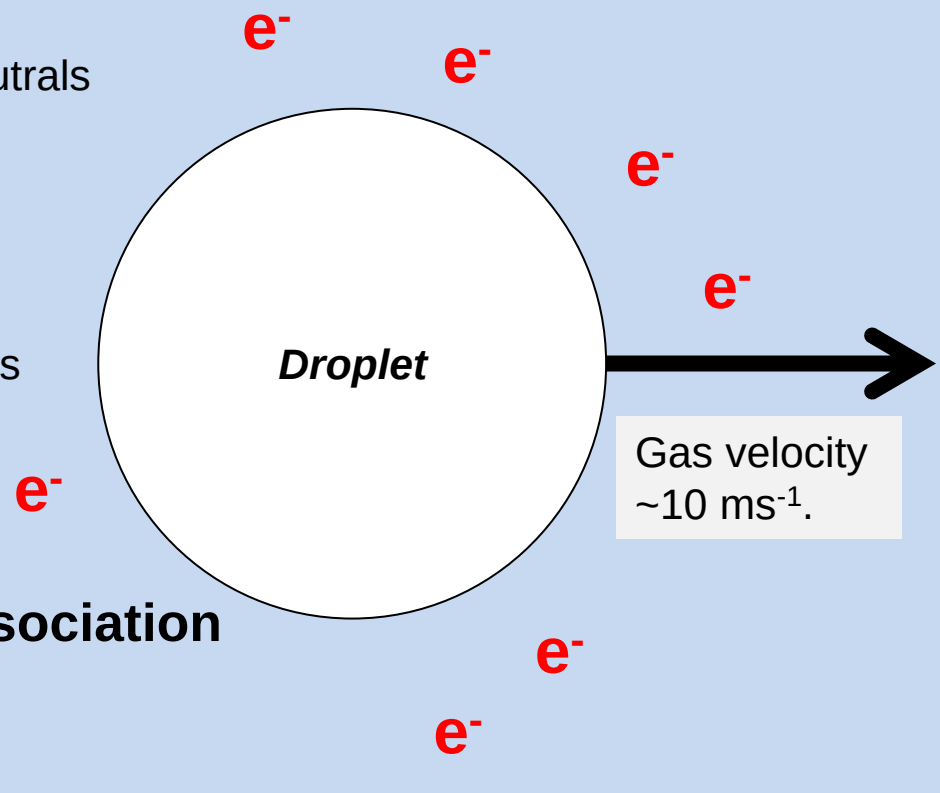

Gas velocity ~10 ms^{-1}.

Water dissociation
$H_xO_y^+$
$O_xH_y^-$

High speed imaging

~ 5 droplets in plasma region at any instant

Plasma region

Droplet Size and Velocity Distributions

pd.maguire@ulster.ac.uk

- Evaporation
  - H2O production rate, delivered into plasma
- Droplet Size Distribution
  - Obtained from imaging in flight
  - 15um (CMD), no plasma

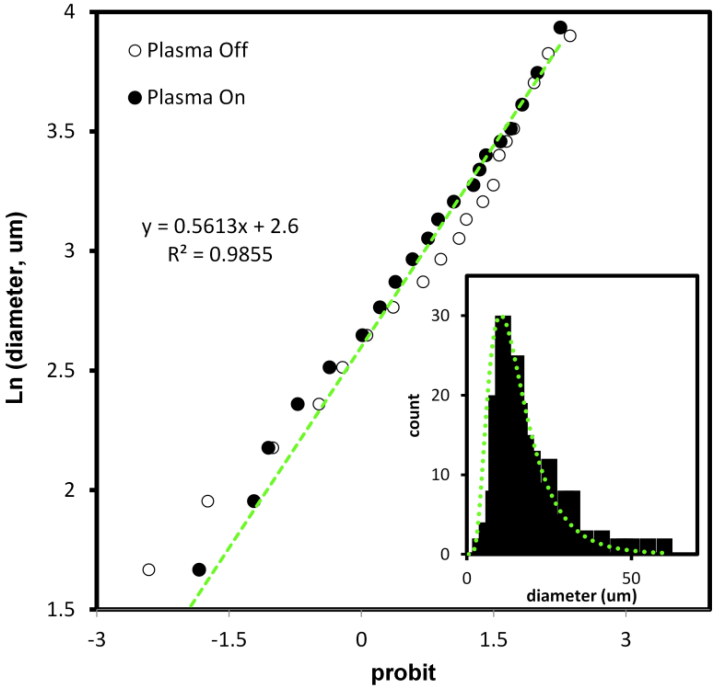

- Velocity Distribution
  - V(r) measured by imaging (but outside tube)
  - Drop travelling at 75% velocity of gas
  - Is this true inside tube?
- Stokes Flow regime
  - Determines whether convection or diffusion carries H2O away from droplet into plasma

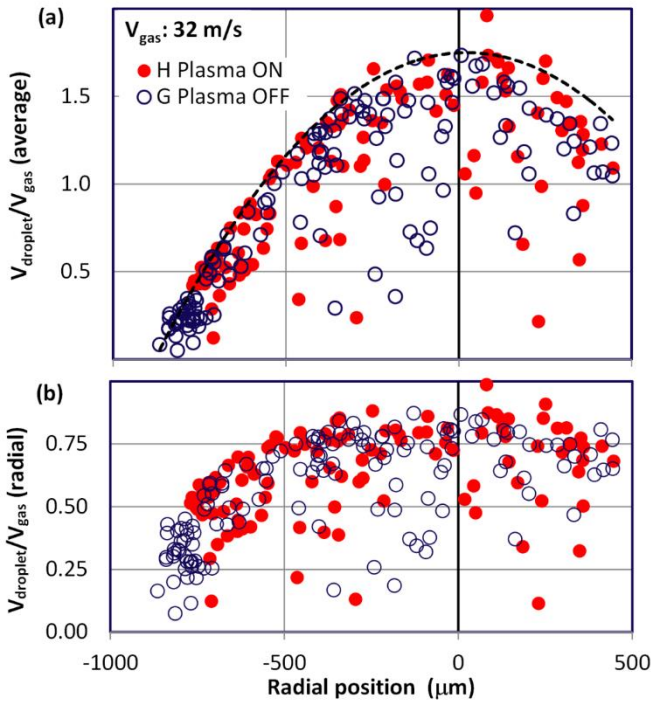

Controlled microdroplet transport in an atmospheric pressure microplasma
P. D. Maguire, C. M. O. Mahony, C. P. Kelsey, A. J. Bingham, E. P. Montgomery, E. D. Bennet, H. E. Potts, D. C. E. Rutherford, D. A. McDowell, D. A. Diver, and D. Mariotti, Appl. Phys. Lett. 106, 224101 (2015), https://doi.org/10.1063/1.4922034

Evaporation

pd.maguire@ulster.ac.uk

RF 13.56MHz
n_e: 10^{12} – 10^{14} cm^{-3}.

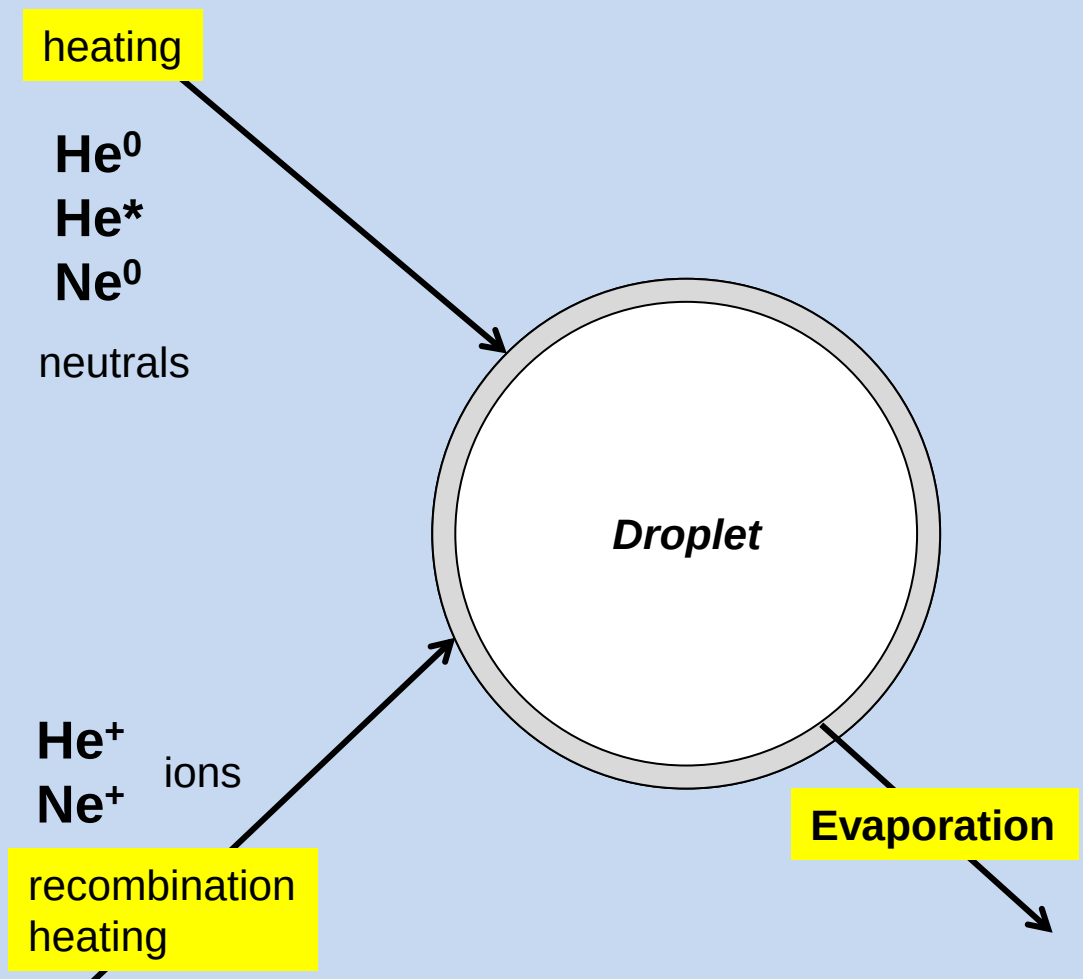

Evaporation
Droplet size
15μm (CMD) → 13μm (CMD)

Evaporation ~ D^2
Average Evaporation rate:
5×10^{-8} m^2 s^{-1}.

Droplet loss by evaporation
Lost: smaller droplets < 4um
~5% of the total droplet number,
~0.05% of the total liquid flow

Humidity
Average humidity increase due to evaporation **< 100ppm**

Plasma region

Plasma – droplet induced effects

pd.maguire@ulster.ac.uk

RF 13.56MHz
n_e: 10^{12} – 10^{14} cm^{-3}.

He^0
He* neutrals
Ne^0

He^+
Ne^+ ions

Water dissociation
$H_xO_y^+$
$O_xH_y^-$

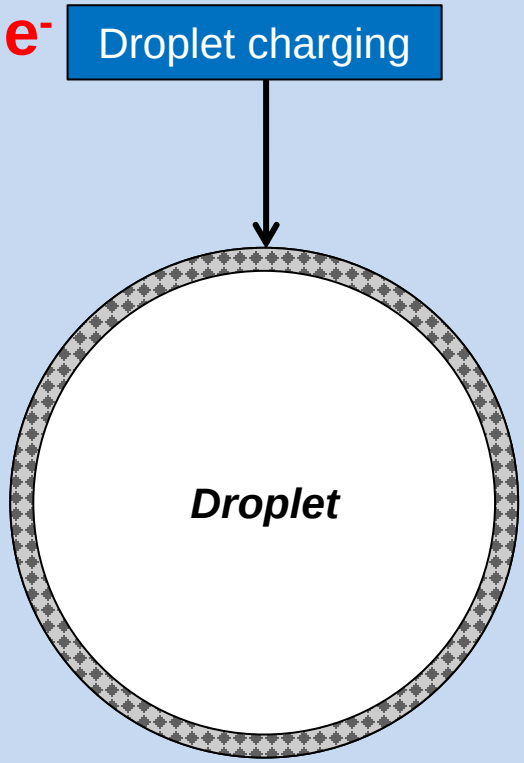

Net electron flux initially
Droplet charges rapidly until it reaches
Negative floating potential
Then electron flux = ion flux
Timescale ns, (ω_i)

Plasma region

Plasma – droplet induced effects

pd.maguire@ulster.ac.uk

RF 13.56MHz
n_e: 10^{12} – 10^{14} cm^{-3}.

He^0
He* neutrals
Ne^0

He^+
Ne^+ ions

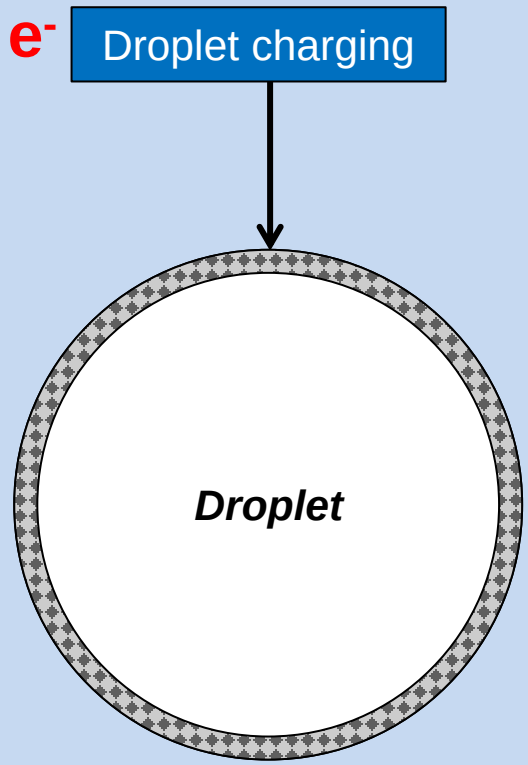

Net electron flux initially
Droplet charges rapidly until it reaches
Negative floating potential
Then electron flux = ion flux
Timescale ns, (ω_i)

Plasma volume ~10^{-8} m^3.
Total no. electrons: > 10^{10}.
Max. electrons lost to droplet 0.1%

Plasma region

Electron flux to droplet

Plasma measurements

pd.maguire@ulster.ac.uk

- Droplet addition
  - Reduction in gas temperature
  - Reduction in plasma volume

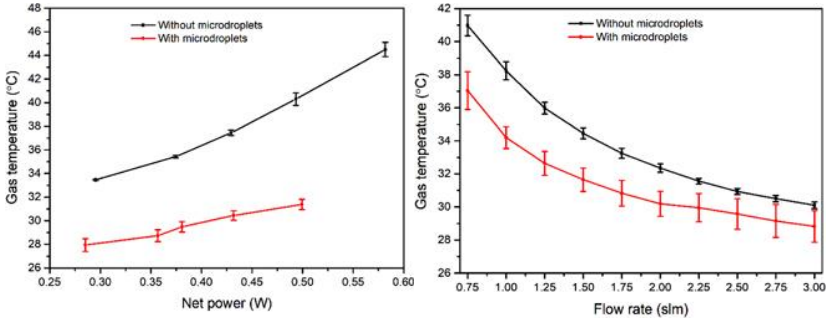

N Hendawy *et al* 2020 *Plasma Sources Sci. Technol.* **29** 085010

- Probe electrodes
  - 0.1 mm diameter
  - 3 mm diameter
  - Located 3 mm – 40 mm from plasma

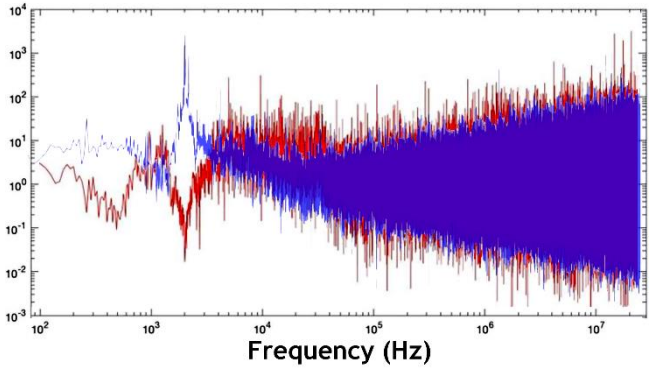

Power spectral density plots from plasma exposed electrode (blue), superimposed on that of plasma with droplets.

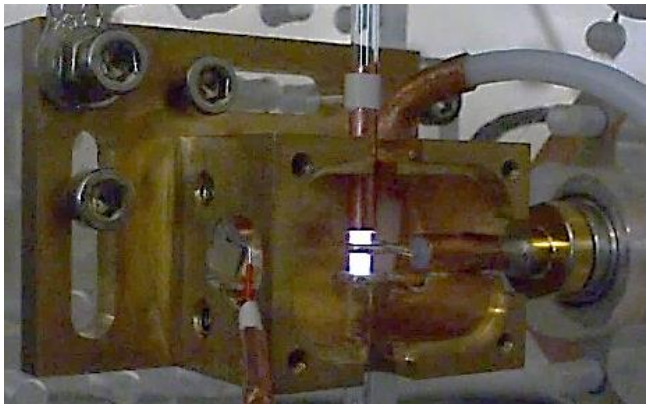

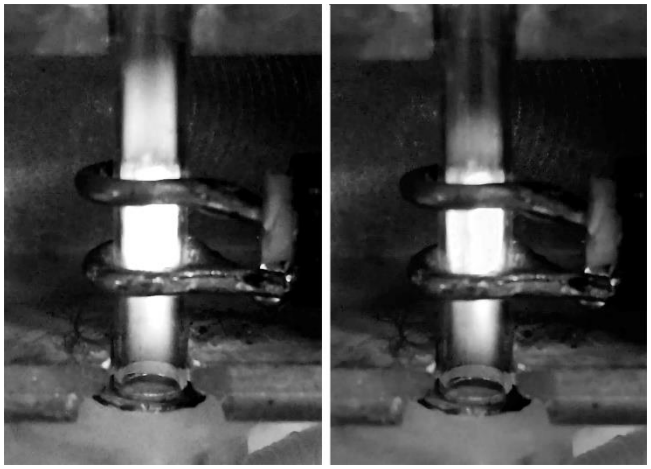

Plasma length between electrodes: 3.5 mm
Distance GND electrode to probe electrode: 3mm
Air gap end of capillary to probe electrode: 0.5 mm
Left: Plasma only. Power (absorbed) 2.7 W
Left: Plasma with droplets. Power (absorbed) 2.9 W

Plasma only

pd.maguire@ulster.ac.uk

- Low power
  - Distance 15 mm from plasma
  - Probe: 0.1 mm
  - Measured probe potential increases with power
  - Probe is outside plasma afterglow region
  - Plasma potential via resistor divider network
  - Probe is not coupled to plasma
- High power
  - Threshold (~1 W)
  - Probe potential decreases with power
  - High negative bias
  - Probe is coupled to plasma

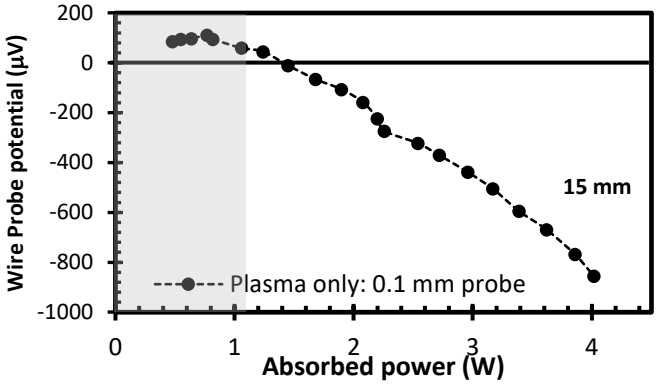

Plasma with droplets

pd.maguire@ulster.ac.uk

- Low power
  - Distance 15 mm from plasma
  - Probe: 0.1 mm
  - Measured probe potential increases with power
  - Probe is outside plasma afterglow region
  - Plasma potential via resistor divider network
  - Probe is not coupled to plasma

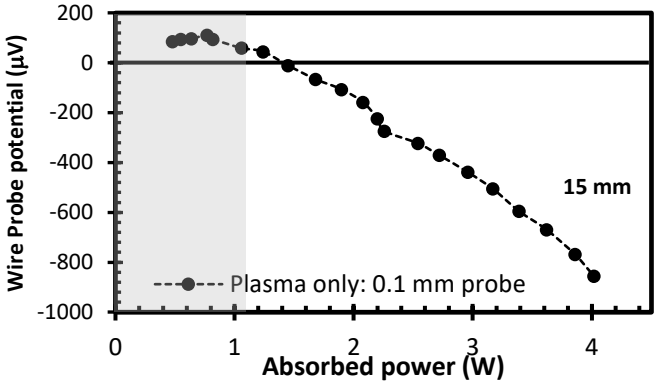

- High power
  - Threshold (~1 W)
  - Probe potential decreases with power
  - High negative bias
  - Probe is coupled to plasma

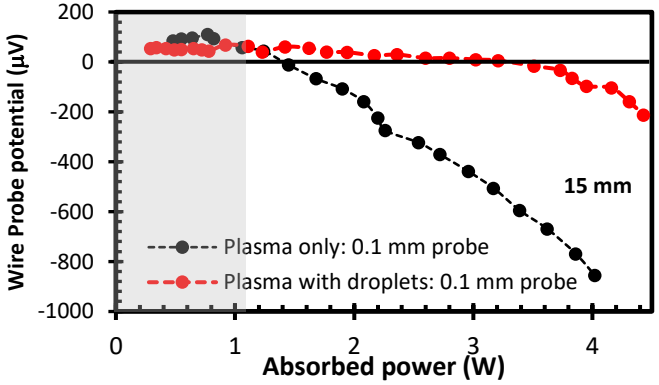

- With droplets
  - Plasma volume is constricted
  - Coupling threshold increases to 3.7 W
  - Droplet impact on probe almost zero

Droplet charge measurement

pd.maguire@ulster.ac.uk

- Large area Probe
  - Diameter: 3mm > plasma diameter (2mm)
  - Droplet impact
  - Below coupling threshold power
- Plasma only
  - reference potential
- Plasma with droplets
  - reference potential and plasma potential induced due to negative droplet charge
  - Average droplet charge: net potential difference and droplet rate
  - Coupling threshold power increases with distance
  - Charge increases with power, decreases with distance

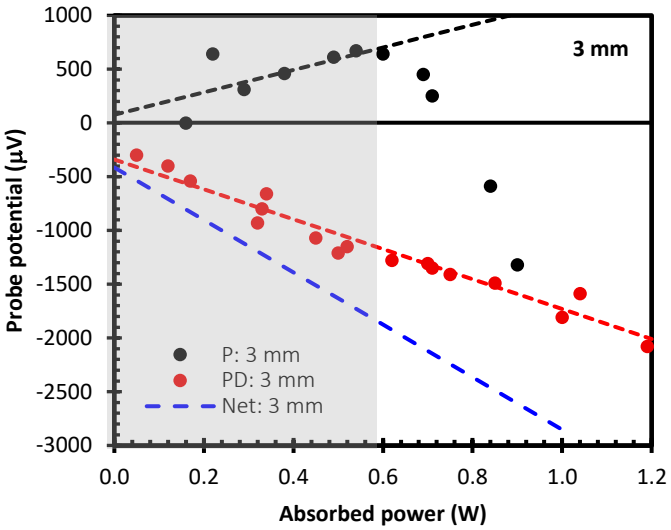

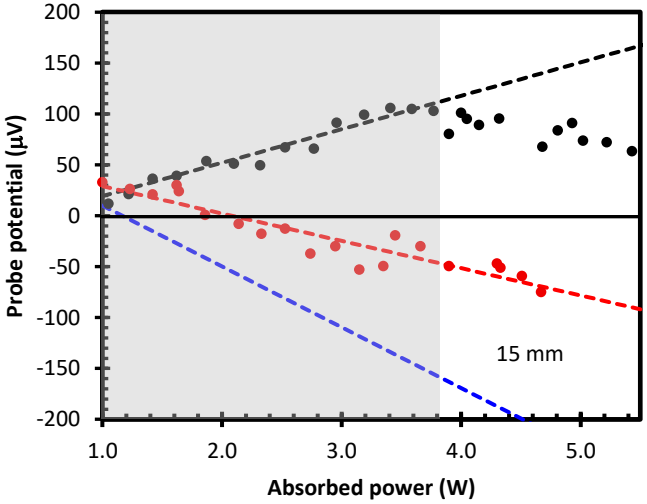

Coupling power

pd.maguire@ulster.ac.uk

- Plasma – Droplets
  - Plasma volume constriction
  - Large gap to probe
  - Higher power required to couple

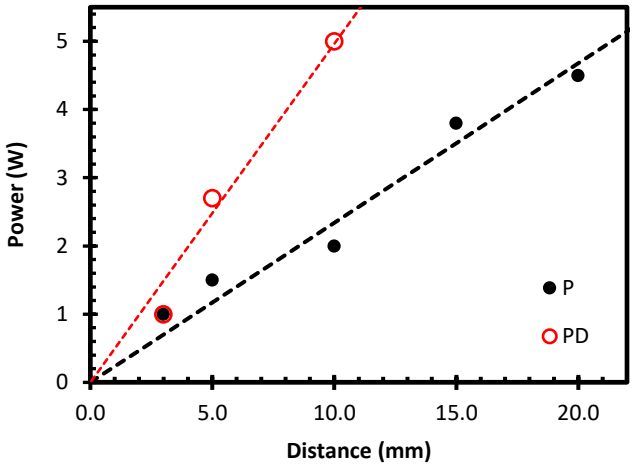

Coupling power

pd.maguire@ulster.ac.uk

- Plasma – Droplets
  - Plasma volume constriction
  - Large gap to probe
  - Higher power required to couple
- Power density
  - Above 5mm distance, required power density is almost constant
  - Power density for droplets x 3 for plasma only
  - Note: 1 – 5 droplets in plasma simultaneously

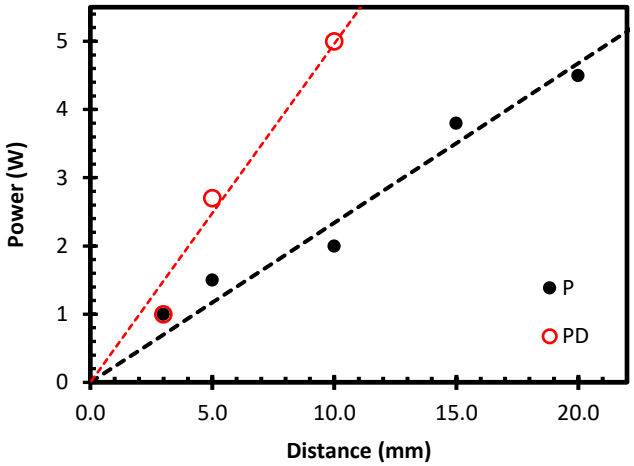

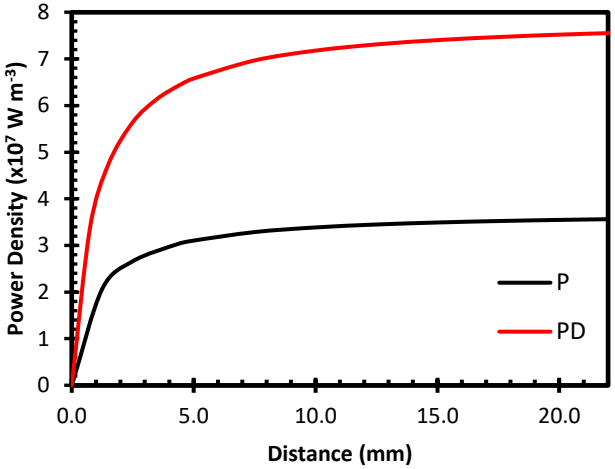

Droplet charge measurement

pd.maguire@ulster.ac.uk

- Large area Probe
  - Diameter: 3mm > plasma diameter (2mm)
  - Droplet impact
  - Below coupling threshold power
- Plasma only
  - reference potential
- Plasma with droplets
  - reference potential and plasma potential induced due to negative droplet charge
  - Average droplet charge: net potential difference and droplet rate
  - Coupling threshold power increases with distance
  - **Charge increases with power, decreases with distance**

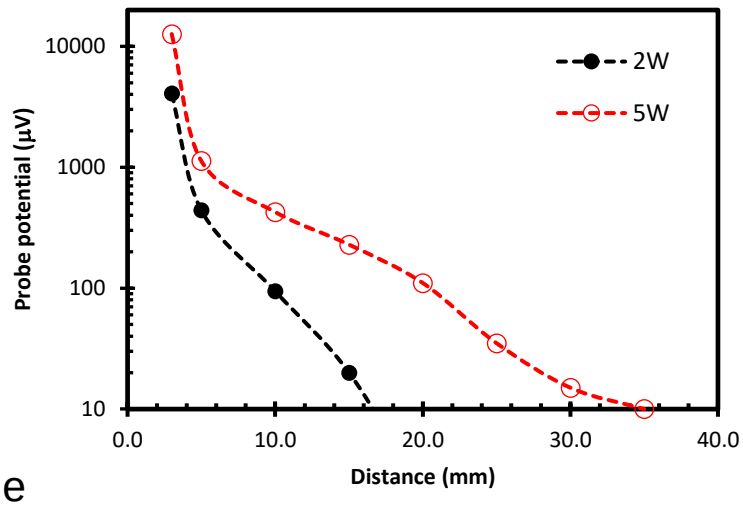

Charge – Net Potential

pd.maguire@ulster.ac.uk

$$i = \frac{dq'}{dt} = \frac{qvR^2}{\sqrt{\left(R^2 + x^2\right)^3}}$$

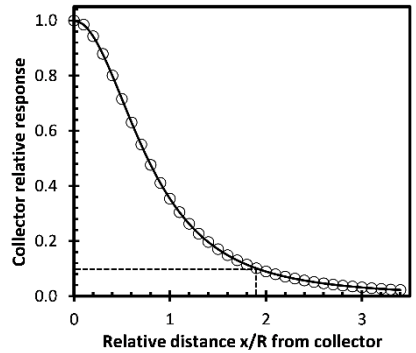

Electrode relative response to charged particle flux versus particle distance, normalised to electrode radius, R.

- Image charge estimate
  - Single charge
  - x: moving droplet distance from probe
  - v: droplet velocity
- Droplet stream
  - Measured characteristics
  - Droplet rate (all sizes) : 5 x 10^4
  - v: average velocity
  - R: electrode radius
  - multiple droplets in probe capture zone

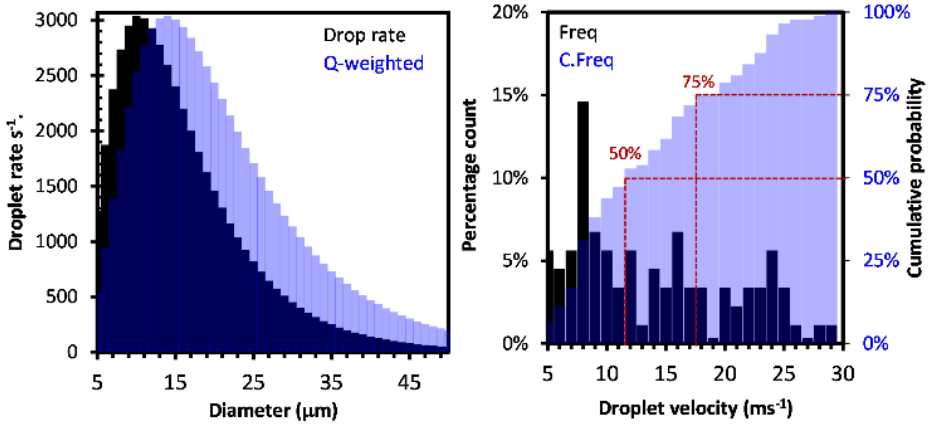

(a) Droplet rate versus size (count median diameter: **13.6 µm**, geometric std. deviation: 1.7) for a total droplet rate of 5 x 10^4 s^{-1}. *Also shown*: equivalent charge contribution, assuming a linear charge – diameter relationship. **60% droplets < 20um**
(b) Droplet velocity distribution and cumulative frequency distribution **showing 50% of droplets travel at ≤ 12 ms^{-1}, and 75% at ≤ 17 ms^{-1}.** The peak and average gas velocities within the capillary are ≤ 16 ms^{-1} and ≤ 32 ms^{-1} respectively, assuming laminar flow.

Probe calibration

pd.maguire@ulster.ac.uk

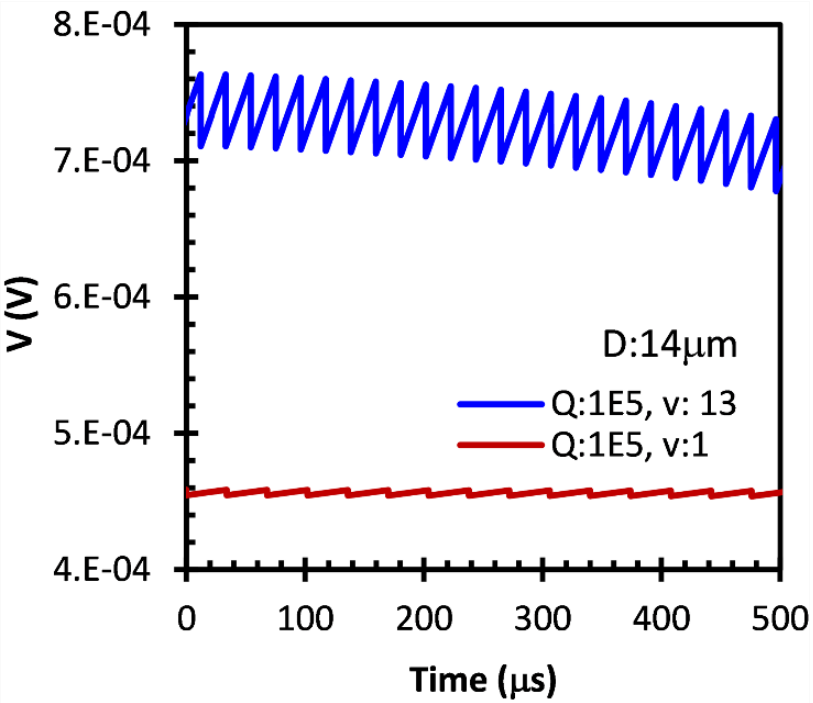

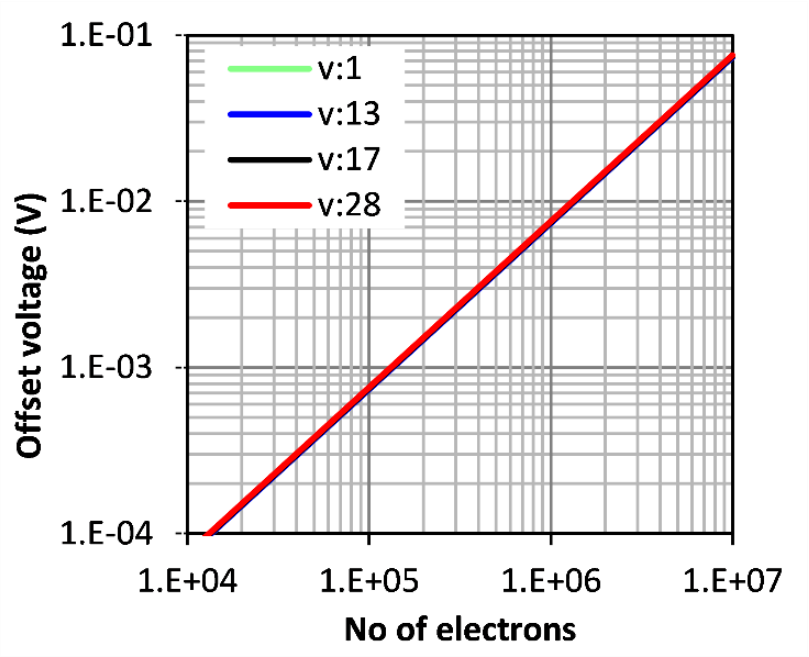

(a) Simulated waveforms for fixed droplet diameter (14 μm) and charge (10^5 electrons) for different velocities

(b) offset voltage versus charge, for different droplet velocities.

Probe bias plus ripple due to individual droplets

Probe bias insensitive to velocity

Probe calibration

pd.maguire@ulster.ac.uk

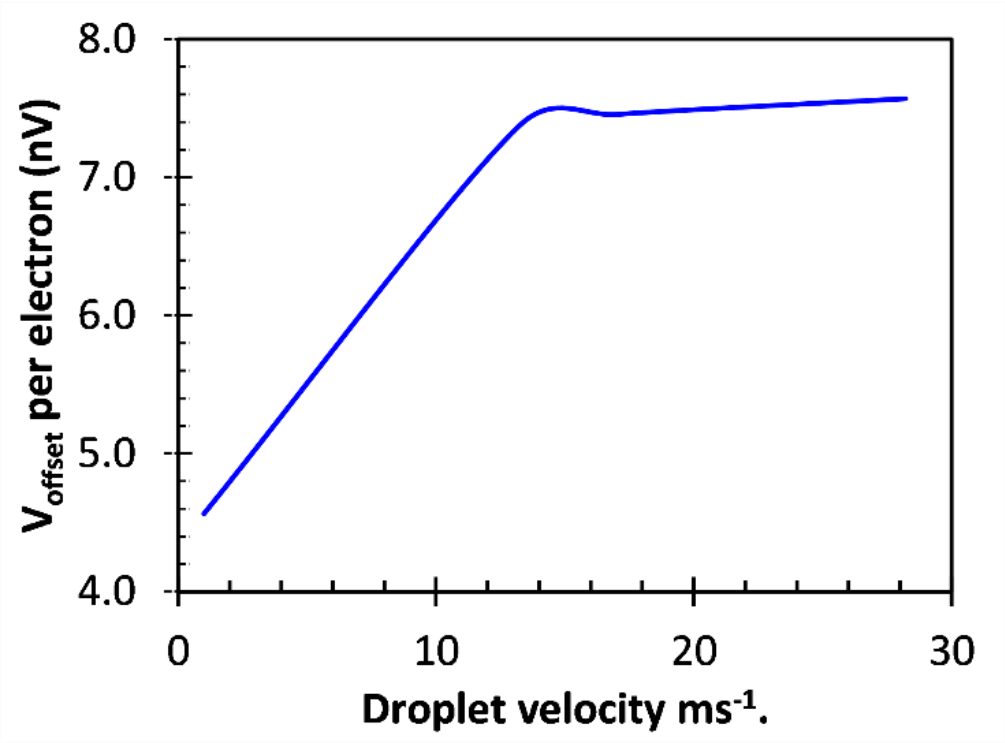

Calculated offset voltage per electron versus velocity.

- The simulation range extended a distance 4 x R from an electrode of radius R.
- The droplet diameter (D) and spacing (G) was 14 μm and v x T_{int} respectively, where T_{int} is the droplet generation interval, 20 μs.
- The minimum no of droplets was 4R/(D+G).

Droplet charge

pd.maguire@ulster.ac.uk

- Within plasma region
  - > 10^6 electrons (1.5 W)
  - > 4 x 10^6 electrons (5 W)

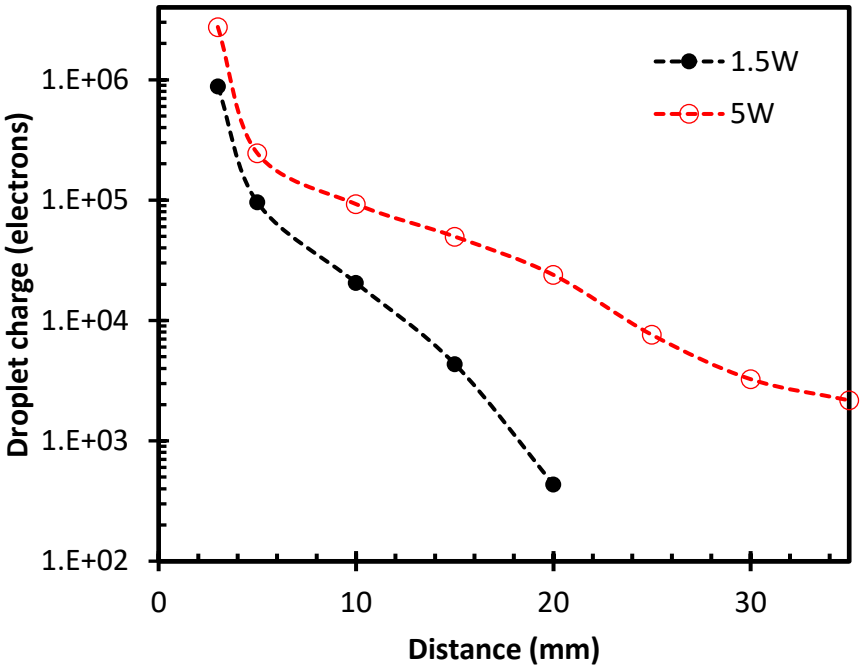

- Rayleigh limit
  - High power
  - Diameters ≤ 15 μm
  - ~60% of droplet count

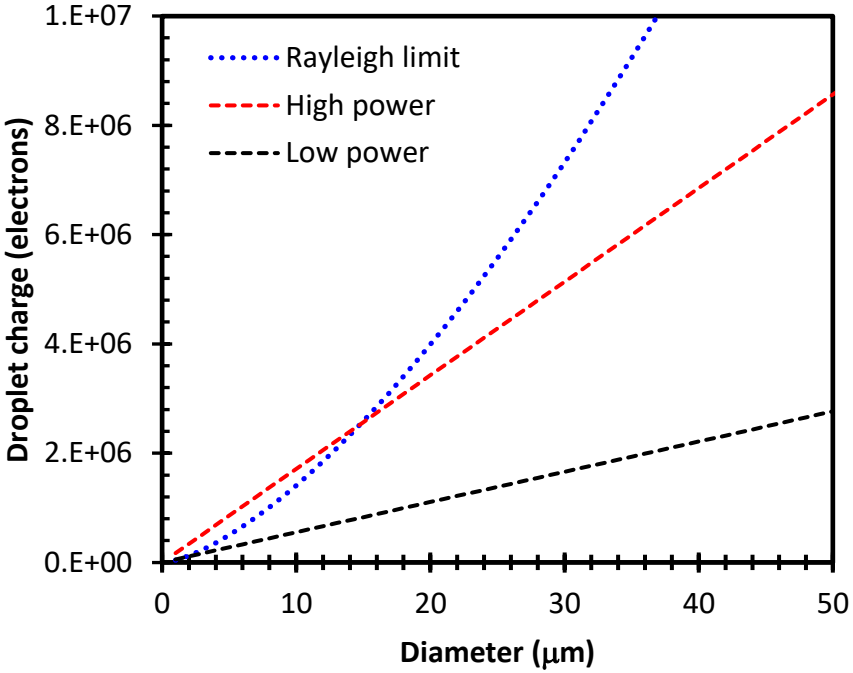

Droplet charge model

Electron flux model

pd.maguire@ulster.ac.uk

Collisional (high pressure) charge flux theory

No analytical solution

Standard orbital motion limited (OML) theory

Collisionless, low pressure approximation - underestimate

Droplet potential obtained by equating ion and electron currents to and from the droplet i.e.

$$\left(\frac{T_e}{m_e}\right)^{1/2}\left[1-\exp\left(-\frac{e|\varphi_s|}{K_B T_e}\right)\right]=\left(\frac{T_i}{m_i}\right)^{1/2}\left(\frac{e|\varphi_s|}{K_B T_i}\right)$$

total flux Γ is given by

$$4\pi r_o^2 Z_i e n_{oi}\left(\frac{K_B T_i}{2\pi m_i}\right)^{1/2}\frac{e|\varphi_s|}{K_B T_i}$$

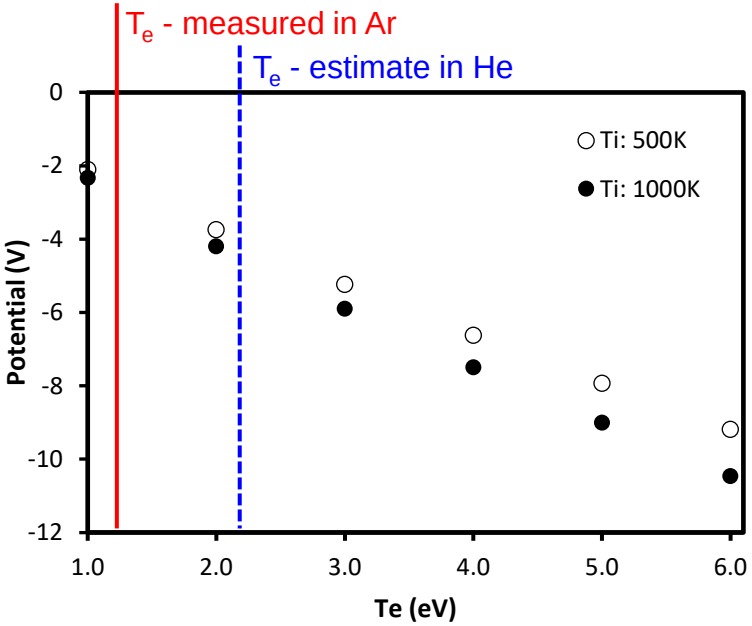

Droplet potential versus electron temperature, for two values of T_i = 500K, and 1000K calculated using Orbital Motion Limited (OML) theory.

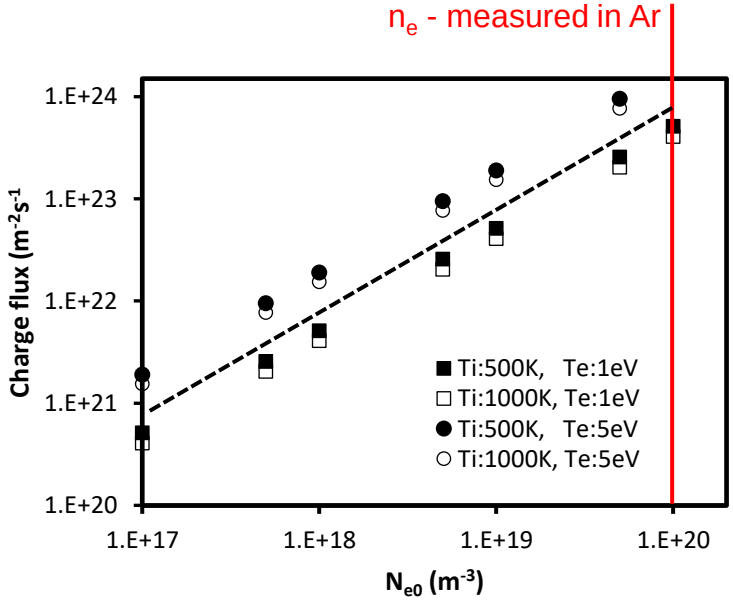

Ion/electron OML flux to 15 μm droplet versus plasma density (n_{e0}) for T_i = 500K, and 1000K and upper/lower values of T_e of 1 eV and 5 eV

Electron density and sheath width

pd.maguire@ulster.ac.uk

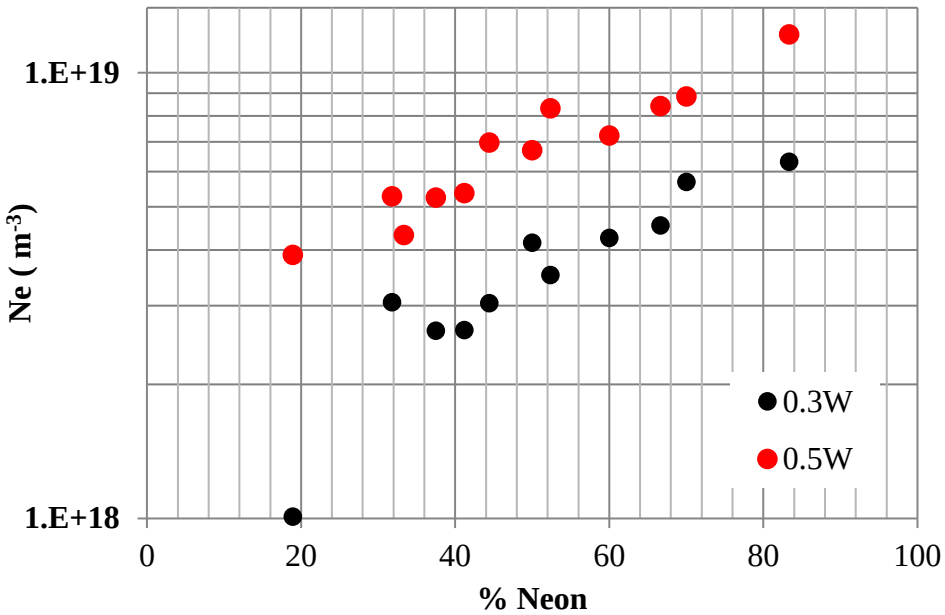

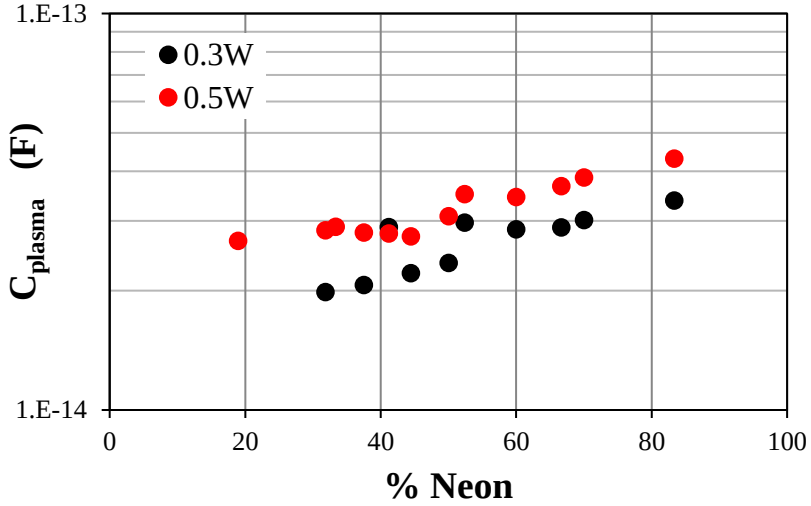

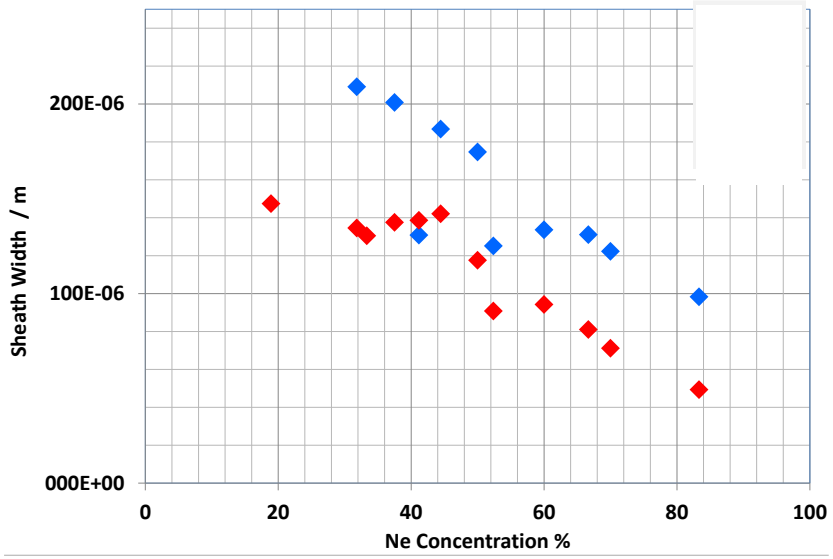

Collisional mobility – impedance model

Impedance, phase measurements

- He 60%, 40% Ne, 0.3W
- **Time Averaged Sheath Width**

Gas ~ 105 μm

Gas & droplets ~ 200 μm

- **Time Averaged Electron Density**

Gas ~ 3×10^{18} m^{-3}

Gas & droplets ~ 7×10^{18} m^{-3}

Electron flux model

pd.maguire@ulster.ac.uk

Collisional (high pressure) charge flux theory

No analytical solution

Standard orbital motion limited (OML) theory

Collisionless, low pressure approximation - underestimate

Droplet potential obtained by equating ion and electron currents to and from the droplet i.e.

$$\left(\frac{T_e}{m_e}\right)^{1/2}\left[1-\exp\left(-\frac{e|\varphi_s|}{K_B T_e}\right)\right]=\left(\frac{T_i}{m_i}\right)^{1/2}\left(\frac{e|\varphi_s|}{K_B T_i}\right)$$

total flux Γ is given by

$$4\pi r_o^2 Z_i e n_{oi}\left(\frac{K_B T_i}{2\pi m_i}\right)^{1/2}\frac{e|\varphi_s|}{K_B T_i}$$

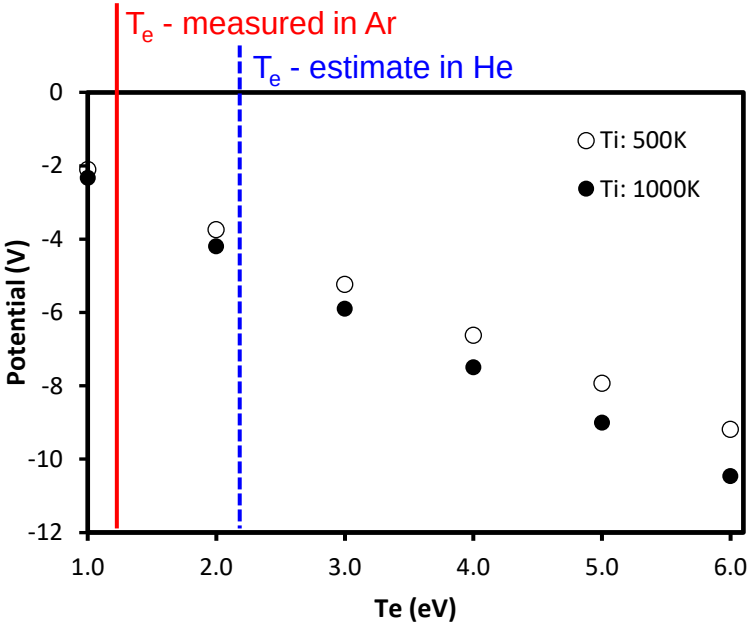

Droplet potential versus electron temperature, for two values of T_i = 500K, and 1000K calculated using Orbital Motion Limited (OML) theory.

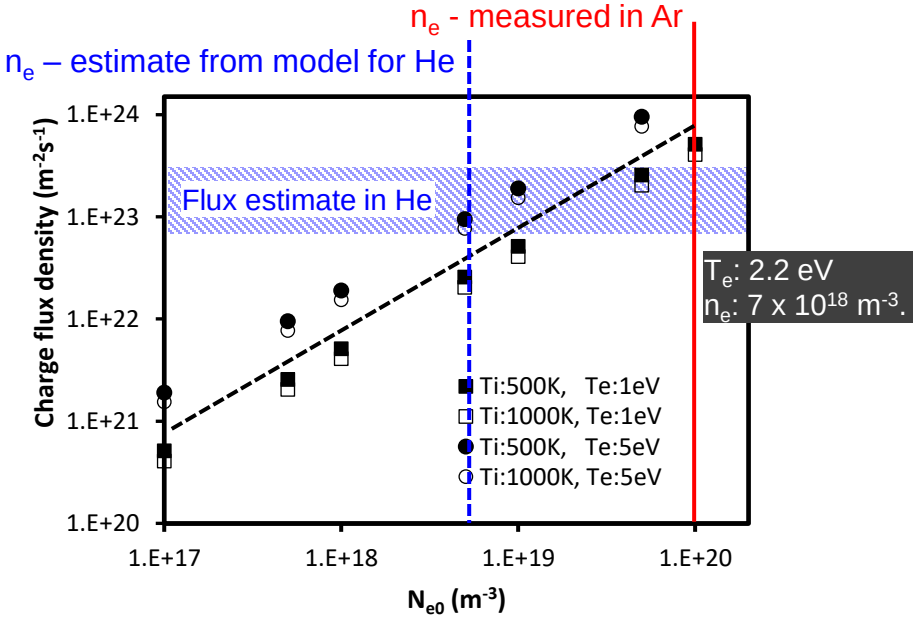

Ion/electron OML flux to 15 μm droplet versus plasma density (n_{e0}) for T_i = 500K, and 1000K and upper/lower values of T_e of 1 eV and 5 eV

Solvated electrons

Flux and charge in a fully collisional plasma

Collisional Plasma

pd.maguire@ulster.ac.uk

- Solvated electrons
  - Electron flux to liquid, electron solvation
  - Bulk liquid
  - Penetration depth ~ 12 nm
  - Surface concentration ~ 1 mM

The solvation of electrons by an atmospheric-pressure plasma
Paul Rumbach, David M. Bartels, R. Mohan Sankaran & David B. Go, *Nat Commun* **6,** 7248 (2015). https://doi.org/10.1038/ncomms8248

- Collisional theory
  - regimes depend on Debye length, sheath width, mean free path, probe diameter
  - approximate analytical solutions available for nanoparticles but not for microparticles

Continuum Theory of Spherical Electrostatic Probes
C. H. Su and S. H. Lam, Phys. Fluids **6**, 1479 (1963), http://dx.doi.org/10.1063/1.1710971

- PIC simulation
  - All physically allowed free parameters
  - electron Debye - body radius ratio, ion - electron temperature ratio, and
  - analytically in rigorously defined asymptotic regimes (weak & strong bias, weak & strong shielding, thin and thick sheath).

Continuum-plasma solution surrounding non-emitting spherical bodies
L. Patacchini *and* I. H. Hutchinson, Phys. Plasmas 16, 062101 (2009)
https://doi.org/10.1063/1.3143038

- Scale lengths
- Reactor
  - 10^{-3}
- Droplet
  - 10^{-5}
- Sheath around droplet?
- Debye length?
- Mean free path
  - 10^{-7}
- Solvated electron layer
  - 10^{-8} to 10^{-9}

Electron flux model

pd.maguire@ulster.ac.uk

High Pressure model (Collisional)

- In high pressure plasmas, ion and electron collisions with neutrals modify the charge flux to the surface.
- Analytic expression for charge flux to a probe is not available.

Model implementations

1. COMSOL fluid model. 1D radial
2. 1D radial analytical / numerical model for both $\lambda_{i,e}$ and $\lambda_{Di,e}$ << D, the droplet diameter, based on mobility/diffusion assumptions
   - e.g. see Patacchini and Hutchinson. "Continuum plasma solution surrounding non-emitting spherical bodies." Physics of Plasmas 16.6 (2009): 062101-16

Model regimes

Weak collisionality:

Ion mean free path λ_i, < Debye length λ_{Di},

Strong collisionality:

Electron mean free path $\lambda_e << \lambda_{De}$.

Particle scaling factors

$R/\lambda_i : R/\lambda_{Di} : R/\lambda_e : R/\lambda_{De}$.

Ion, electron temperatures

Inferred from measurements in Ar

Electron, ion density

From collisional – impedance model

$$\nabla\left(-\frac{\partial n_i}{\partial r} - \frac{1}{\tau} n_i \frac{\partial \phi}{\partial r}\right) = 0$$

$$\nabla\left(-\frac{\partial n_e}{\partial r} + n_e \frac{\partial \phi}{\partial r}\right) = 0$$

$$\nabla\left(\frac{\partial \phi}{\partial r}\right) - \frac{1}{\lambda_{De}^2}(n_e - n_i) = 0$$

$$\nabla(x) = 1/r^2 \partial/\partial r(r^2 x)$$

$$\Gamma_i^p = \frac{N_\infty D_i}{R_p}\frac{\partial n_i}{\partial r}(r_p)$$

$$\Gamma_e^p = (N_\infty D_e/R_p)\partial n_e/\partial r(r_p)$$

Plasma charging, collisional model

pd.maguire@ulster.ac.uk

- Plasma – droplet collisional model

  $\lambda_e << \lambda_{De}$. λ_{De}. << r_{NP}.

- Highly collisional
  - Hydrodynamic solution
  - Simulations
  - Asymptotic analytical approximations

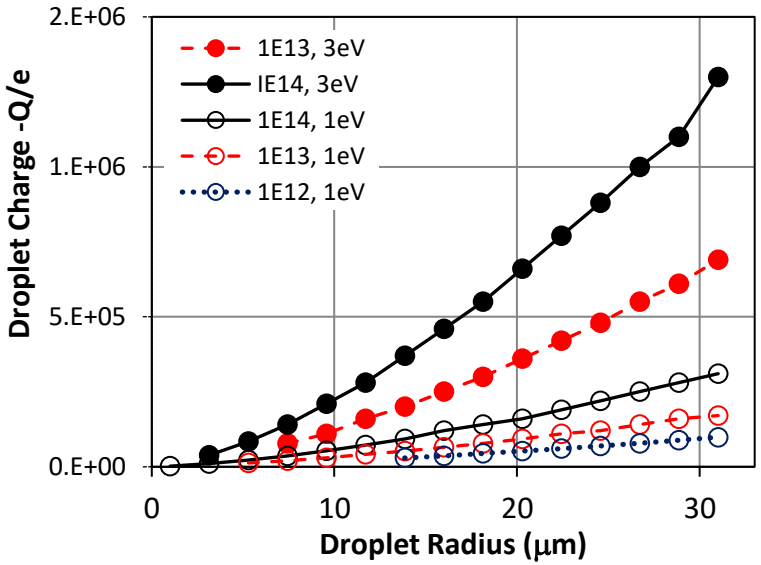

- Model Output
- Q_{drop} v R_{drop}
  - n_e:1x10^{12} – 1x10^{14} cm^{-3}.
  - Average R: Q_d = ~10^5e
  - R = 13 um: Q_d = 5 x10^4e – 2 x10^5e
  - ***Electron flux***
  - 10^{20} – 5 x 10^{23} m^{-2} s^{-1}
  - **Measured charge significantly higher than model**

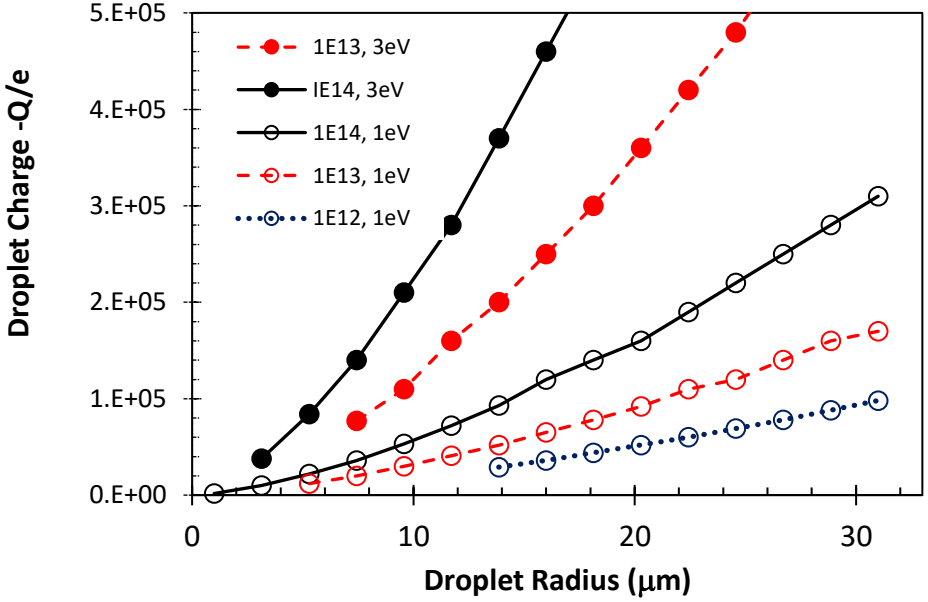

COMSOL: Ne, Ni, potential and flux in sheath

pd.maguire@ulster.ac.uk

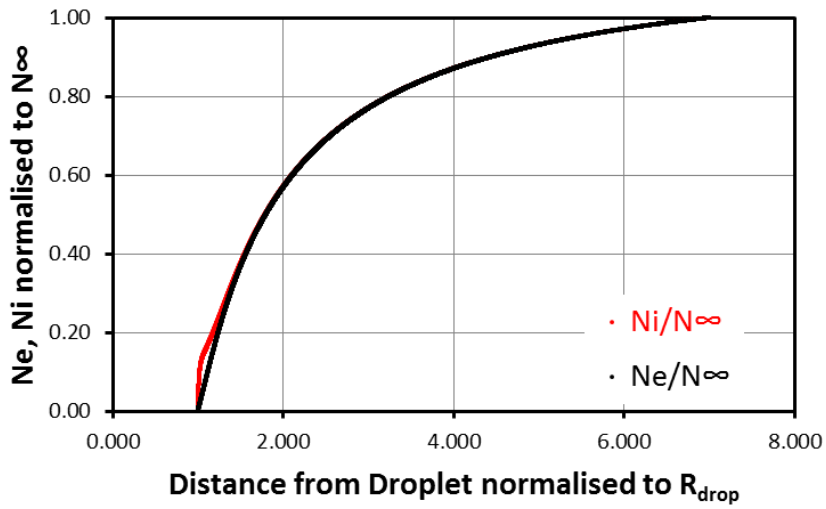

Input parameters

Small Q, low bias

$Q_{drop} = 4 \times 10^5$ e

$T_e = 1$eV

$\phi = -1$

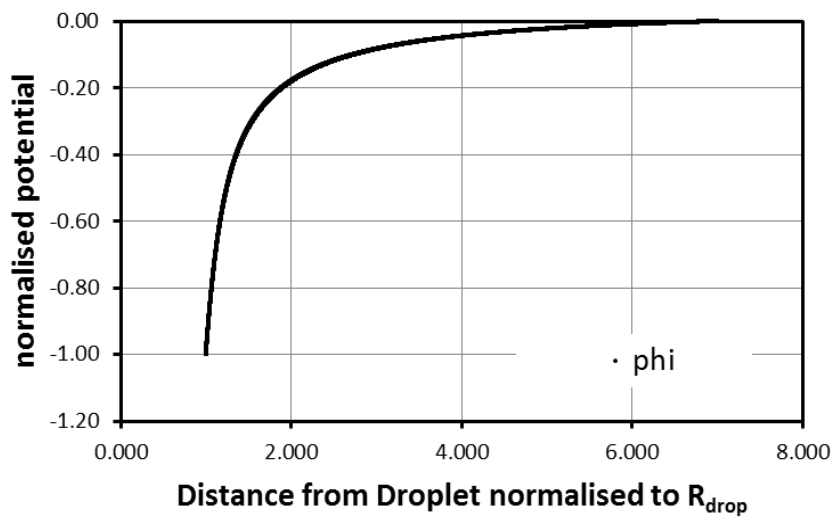

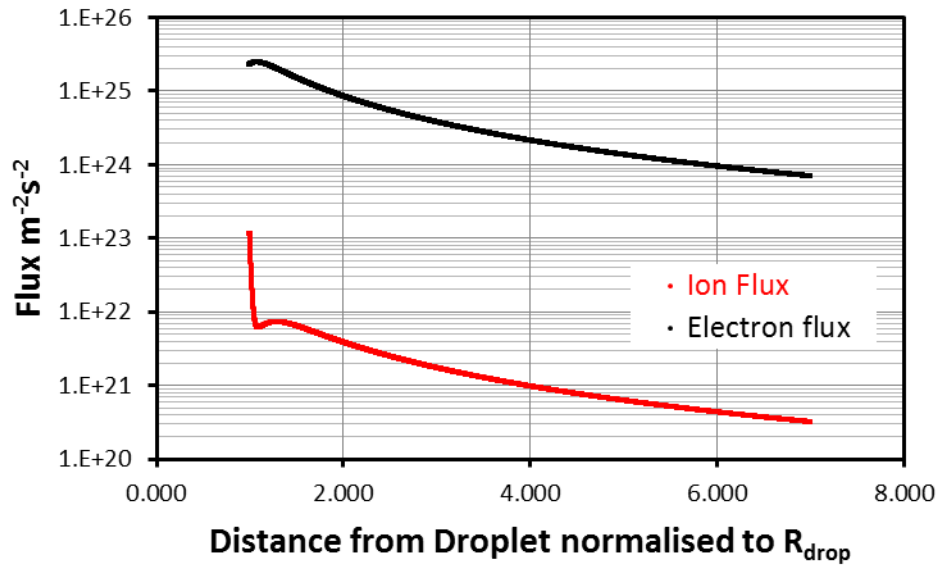

COMSOL Ne, Ni, potential and flux in sheath

pd.maguire@ulster.ac.uk

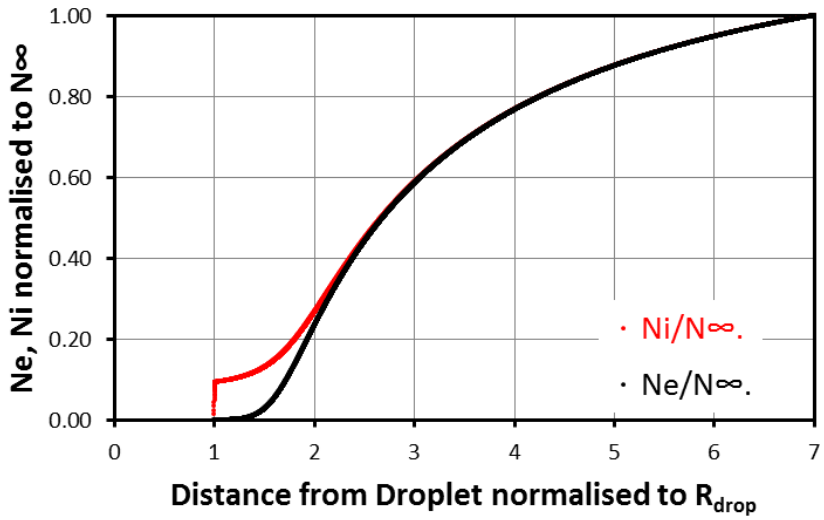

Input parameters

High Q, high bias

$Q_{drop} = 5 \times 10^6$ e

$T_e = 1$eV

$\phi = -11$

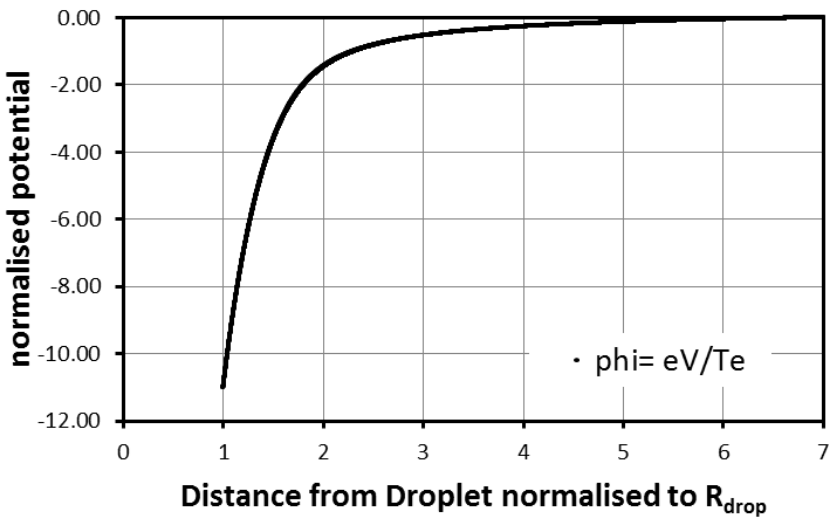

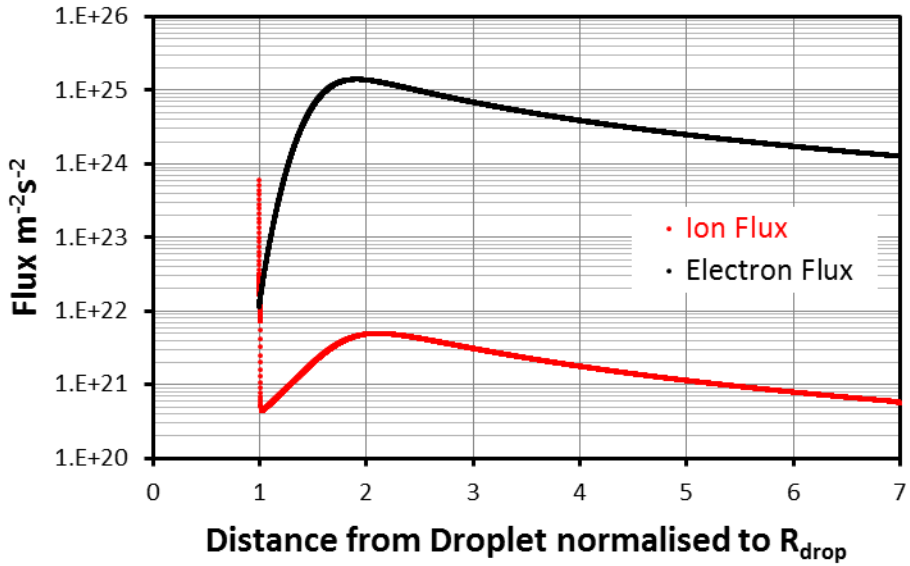

Droplet in plasma charge comparisons

pd.maguire@ulster.ac.uk

- Dusty plasma
  - Low pressure
  - Crystal, levitation
  - 4500e for 10 μm particle
  - Trottenberg et al. 1995
- Unipolar corona charging

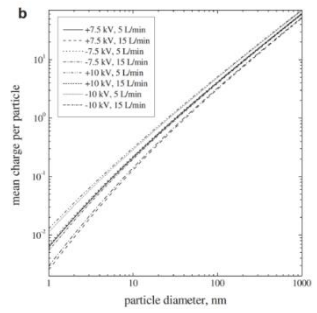

Fig. 8. Variation of mean charge per particle with particle diameter at different aerosol flow rate and applied voltage (a) 0 V and (b) 310 V.

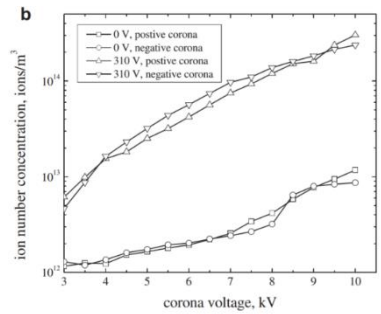

Fig. 5. Variations in ion number concentrations with corona voltage in the charger (a) discharge zone and (b) charging zone.

Corona discharge in a cylindrical triode charger for unipolar diffusion aerosol charging, P. Intra, J. Electrostat. **70** (2012) 136

Simulation: 10um particles,
Q_d = **7000** (8 kV), 3000 (5kV)

Measured: 1um particles,
Q_d = **68** (5kV)

Design of a unipolar aerosol charger to generate highly charged micron-sized aerosol particles. *J Park et al., J. Electrostat.* ***69*** *(2011) 126*

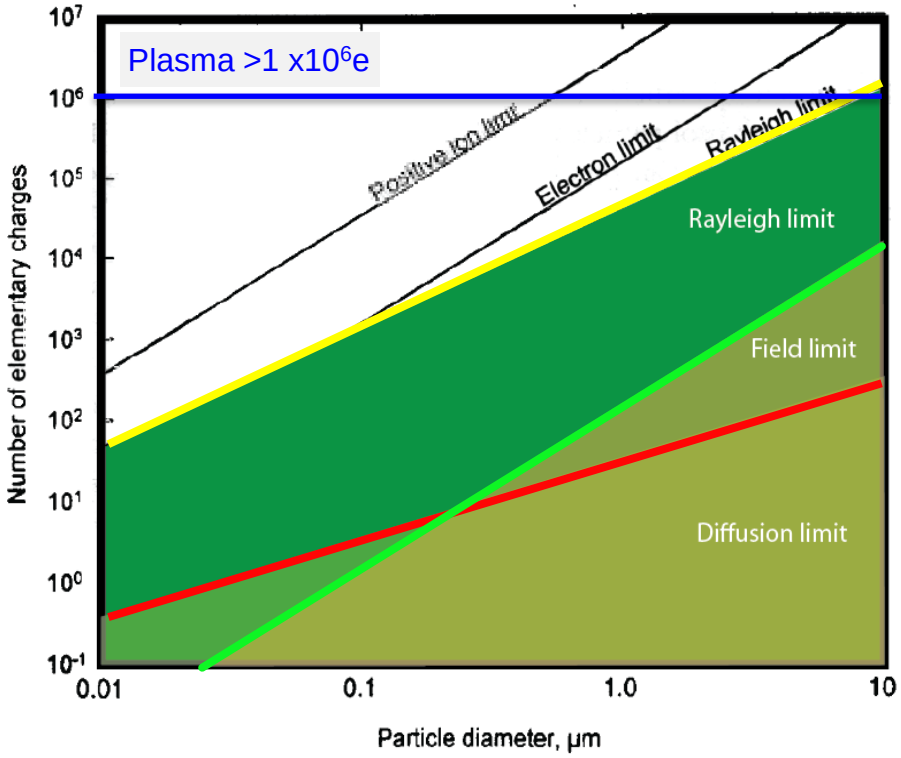

High electron density non-equilibrium atmospheric pressure plasma
Unipolar charging
(T_e >> T_{gas})
X 100 compared to other techniques
Close to Rayleigh limit

Plasma versus Radiolysis or e-Beam

pd.maguire@ulster.ac.uk

- X 10^3 – 10^7 faster
  - **Similar dose rate as gamma radiation**
- Plasma-droplet
  - Dose rate assuming **x%** plasma energy delivered to drop according to ratio VOL_{drop} / VOL_{plasma}
  - 5×10^{-2} kGy s^{-1}.
- Solvated Electron Reduction Hypothesis
  - Reactions: 2nd order
  - Droplet negatively charged
  - **Electrons arrive with very low energy**
  - **Electrostatically confined**
  - **shallow surface layer**
  - Very high local concentration

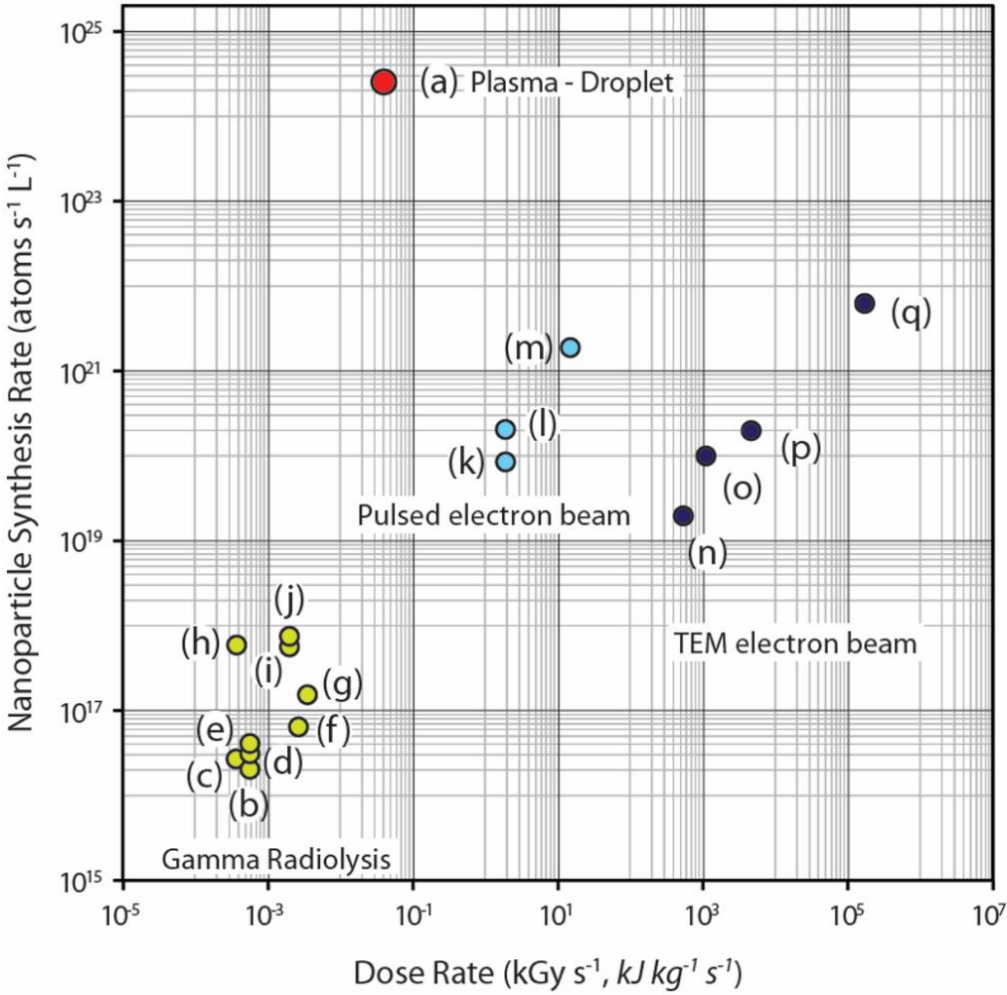

$HAuCl_4$. The reduction of **Au^{III}** proceeds via reactions as:

II	$Au^{III}Cl_4^- + e_{aq}^- \rightarrow Au^{II}Cl_4^{2-}$	(R1)
III / I	$2\ Au^{II}Cl_4^{2-} \rightarrow Au^{III}Cl_4^- + Au^{I}Cl_2^- + 2Cl^-$	(R2a)
0	**$Au^{I}Cl_2^- + e_{aq}^- \rightarrow Au^{0}Cl_2^{2-}$**	**(R3)**
I / II	$Au^{III} + Au^0 \rightarrow Au^{I}$ and Au^{II}	(R4)

Continuous In-Flight Synthesis for On-Demand Delivery of Ligand-Free Colloidal Gold Nanoparticles, Maguire et al., Nano Letts., 2017, https://dx.doi.org/10.1021/acs.nanolett.6b03440

Plasma induced liquid chemistry in droplet

Simulation

Simulation

pd.maguire@ulster.ac.uk

- Electron Flux to droplet
  - Collisional
  - D >> λ_i, D >> λ_{De}.
  - No analytical solution
- Ion Flux to droplet
  - No analytical solution
  - Collisional
  - Very low energy
- Ion type
  - Water product ions
  - Noble gas ions
  - Ratio water/noble ions: important
- Flux induced droplet chemistry
  - Charge and chemical species flux to droplet
- Model (liquid)
  - Plasma induced chemistry
  - In liquid
  - 1D radial
  - 15 species, including solvated electrons
  - 100 reactions
- Charge flux (variable n_e)
- Neutral chemical flux
  - OH, H, H2O2, H2, O2.
- $H_2O \rightarrow H_2O_2$ conversion efficiency
  - Literature, up to 6000ppm
  - Across plasma types and conditions
  - Y_{H2O2} ~10^{-3}, from gas phase measurements
  - Y_{H2O2} ~10^{-4}, from liquid measurements
- $H_2O \rightarrow$ OH, H conversion efficiency
  - OH + OH $\rightarrow H_2O_2$.
  - but some show $N_{OH} \sim N_{H2O2}$

Droplet simulation: H_2O_2, OH

pd.maguire@ulster.ac.uk

Diameter
15um, 20um

Electron flux:
10^{20} – 10^{23} m^{-2} s^{-1}.

H_2O_2:
Decreases with increasing electron flux

OH:
Optimum flux at 10^{22} m^{-2} s^{-1}.

15um: 1mM max conc. Decays by 10^{-4} over 1500nm

20um: 1μM max conc. Decays by 10^{-4} over 2500nm

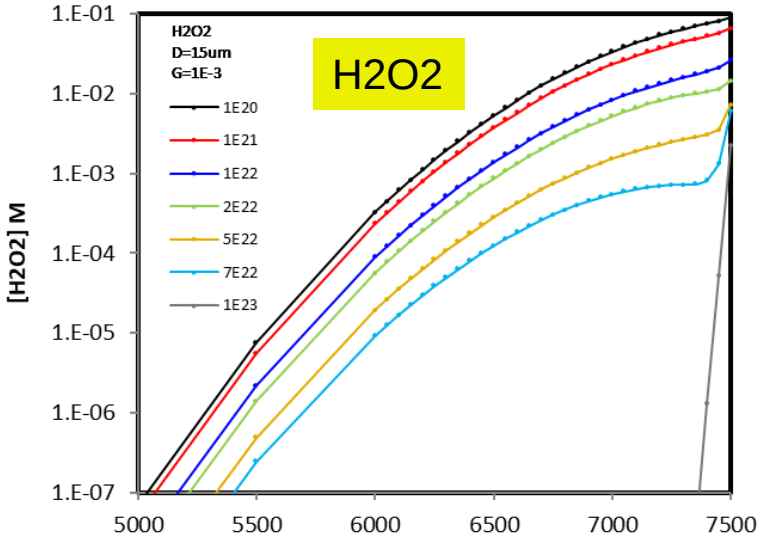

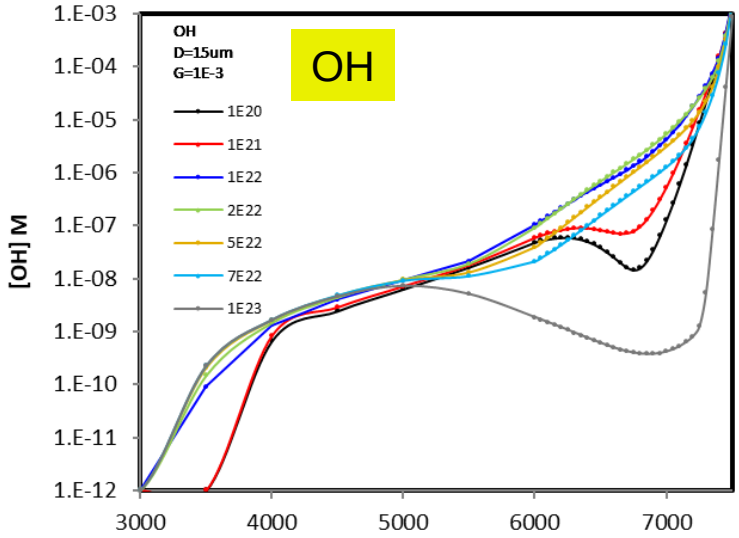

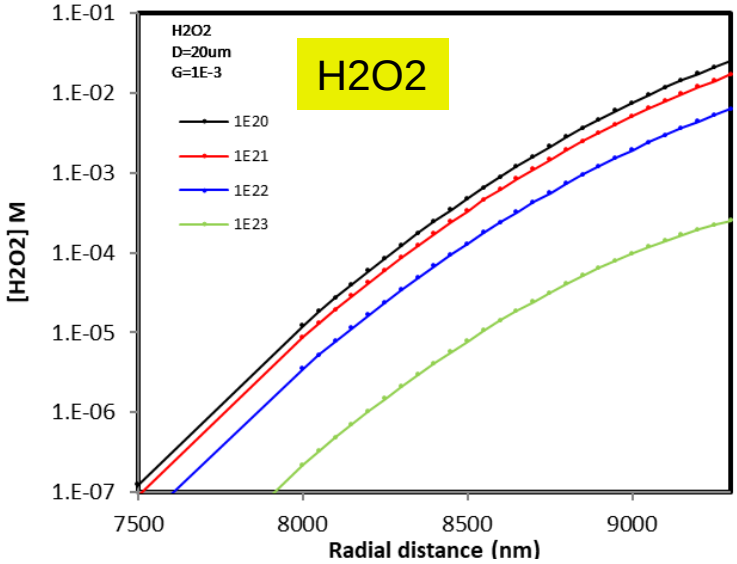

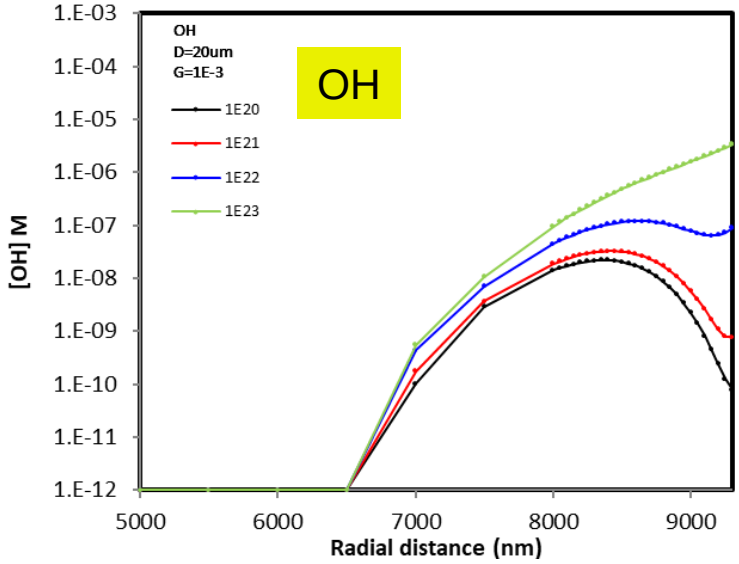

Droplet simulation: solvated electrons

pd.maguire@ulster.ac.uk

Diameter
15um, 20um

Electron flux:
$10^{20} – 10^{23}$ m^{-2} s^{-1}.

H_2O_2:
Decreases with increasing electron flux

OH:
Optimum flux at 10^{22} m^{-2} s^{-1}.

15um: 1mM max conc. Decays by 10^{-4} over 1500nm

20um: 1μM max conc. Decays by 10^{-4} over 2500nm

Solvated electrons
- No electric field in model

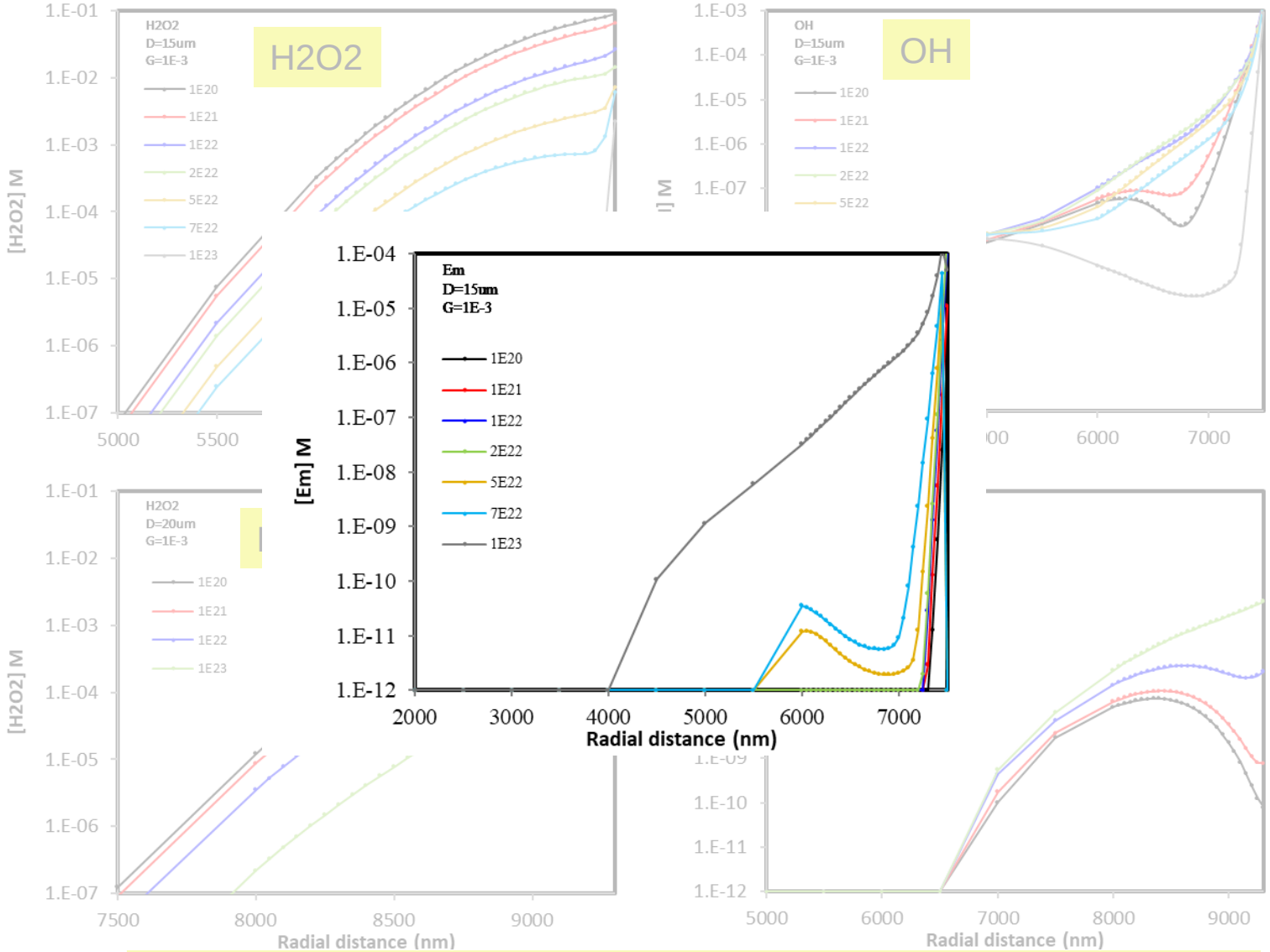

Droplet temperature dependent Henry's constant for OH and H2O2

Some scientific questions

Solvated electron layer

pd.maguire@ulster.ac.uk

- Electron solvation layer
  - Charge: 10^6 electrons: 10 - 20 μm sphere
  - Assume solvation
  - Steady-state, during plasma residence, 100 μs.
  - Unlike radiolysis (transient spurs)
- Estimates from plasma - bulk liquid
  - *Rumbach et al., Nature Comms* **6**, 7248 (2015) Planar plasma – bulk liquid studies:
  - Solvated electron concentration – approaching **1 mM**. *Estimate.*
  - Electron penetration depth **10 nm**
- Surface water structure
  - Water structure with such a high concentration of solvated electrons?
  - Solvation cage: solvated electron surrounded by tetrahedral 4x H_2O molecules.

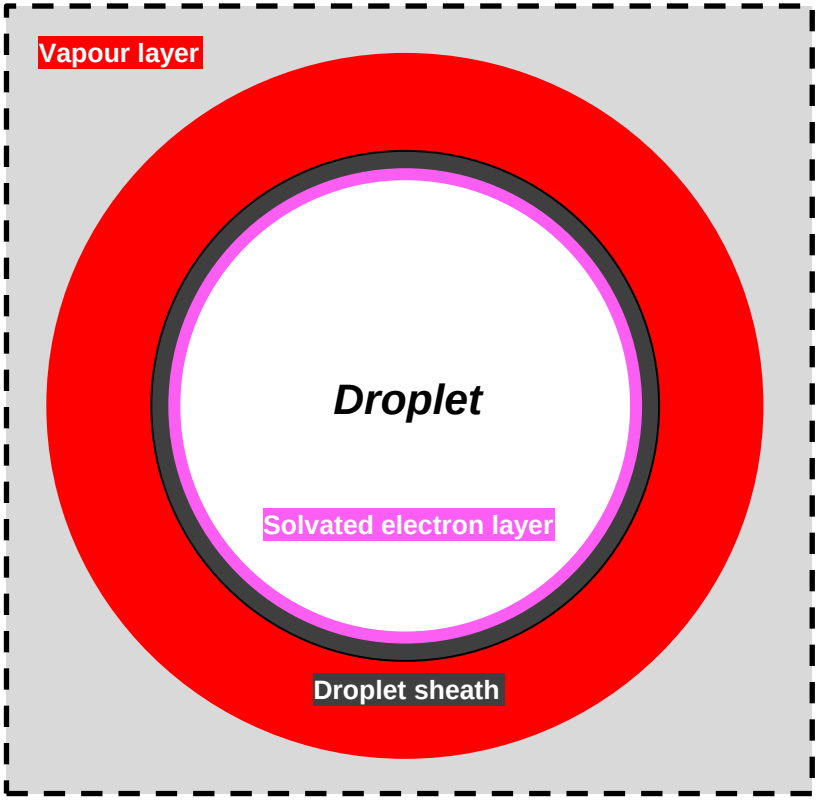

Solvated electron layer

pd.maguire@ulster.ac.uk

- Charged droplet
  - Surface layer of solvated electrons
- Electric field
  - Internal electric field, will develop over time
  - **Dielectric relaxation**
  - Dielectric relaxation time ~50 ms for 15 μm droplet ($\tau_d = \varepsilon/en\mu$)
  - Plasma residence time: 100 μs.
  - **Ion drift**
  - Mobile ion drift (H^+, OH^- from pH).
  - The H^+ diffusion constant is 9×10^{-9} m^2s^{-1} and the time taken to traverse the droplet from centre is ~6 ms.
- Chemical reactions
  - electron initiated
  - pH gradient
  - ion recombination

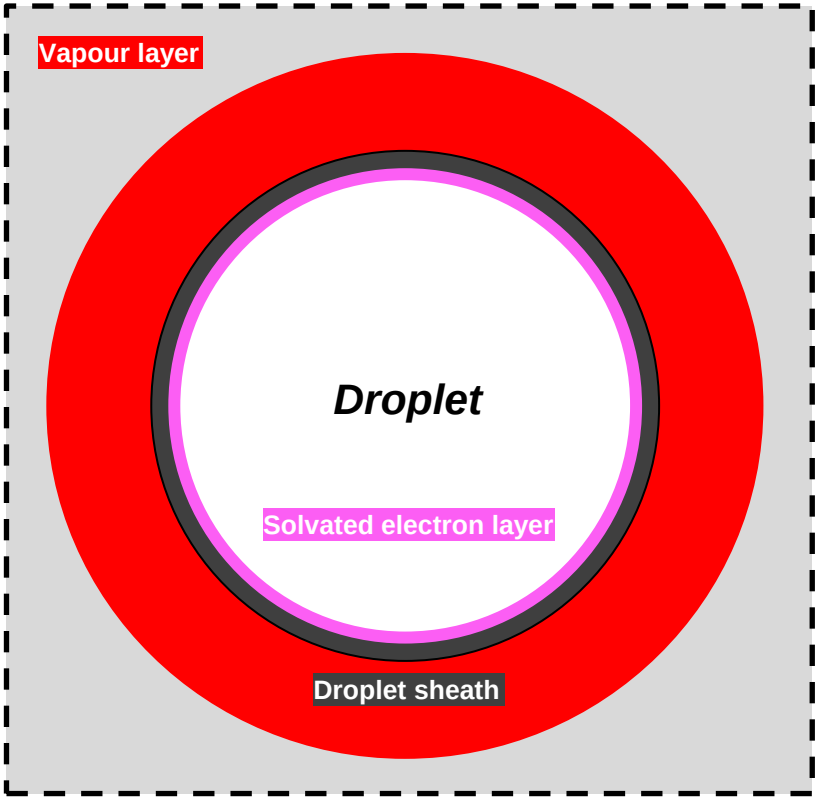

Solvated electron layer

pd.maguire@ulster.ac.uk

- Charged droplet
  - Surface layer of solvated electrons
- Electric field
  - Internal electric field, will develop over time
  - **Dielectric relaxation**
  - Dielectric relaxation time ~50 ms for 15 μm droplet ($\tau_d = \varepsilon/en\mu$)
  - Plasma residence time: 100 μs.
  - **Ion drift**
  - Mobile ion drift (H^+, OH^- from pH).
  - The H^+ diffusion constant is 9×10^{-9} m^2s^{-1} and the time taken to traverse the droplet from centre is ~6 ms.
- Charge separation
  - DI water (pH = 7), total number of H^+ ions in a 15 μm diameter droplet is ~10^5
  - Similar to surface charge magnitude.
  - If all the H^+ ions collect within λ of the surface, to screen negative surface charge
  - All OH^- is displaced to within region λ to 2λ where 2λ < R,
  - Core region (0 → R – 2λ) is depleted of ions .

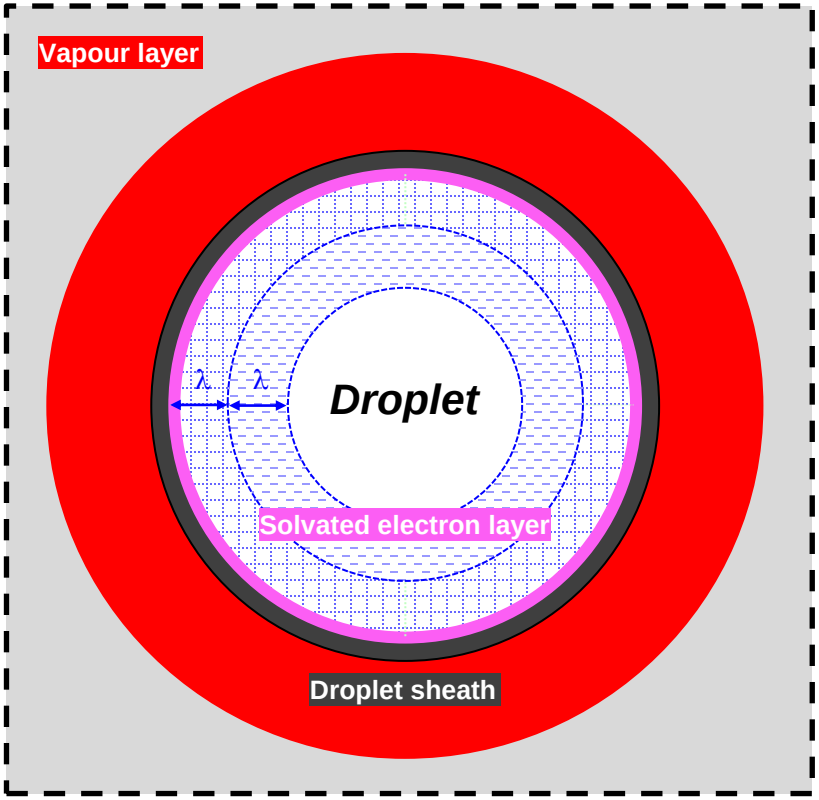

Solvated electron layer

pd.maguire@ulster.ac.uk

- Charged droplet
  - Surface layer of solvated electrons
- Charge separation
  - DI water (pH = 7), total number of H^+ ions in a 15 μm diameter droplet is ~10^5
  - Similar to surface charge magnitude.
  - If all the H^+ ions collect within λ of the surface, to screen negative surface charge
  - All OH^- is displaced to within region λ to 2λ where 2λ < R,
  - Core region (0 → R – 2λ) is depleted of ions
- Debye-Huckel Theory
  - Surface electron charge attracts H^+ into Debye layer λ_1 and repels OH^- into Debye layer λ_2. λ is Debye screen length given by

$$\lambda^2 = \frac{\varepsilon k_B T}{e^2 n}$$

  - n is the charge density. Total net charge within mantle is equal to $-Q_s$, the surface charge.
- Model simulation
  - Debye-Huckle assumes linear Poisson-Boltzmann ie. **V ~ kT/e**.
  - However estimated droplet potential: **- 10V**

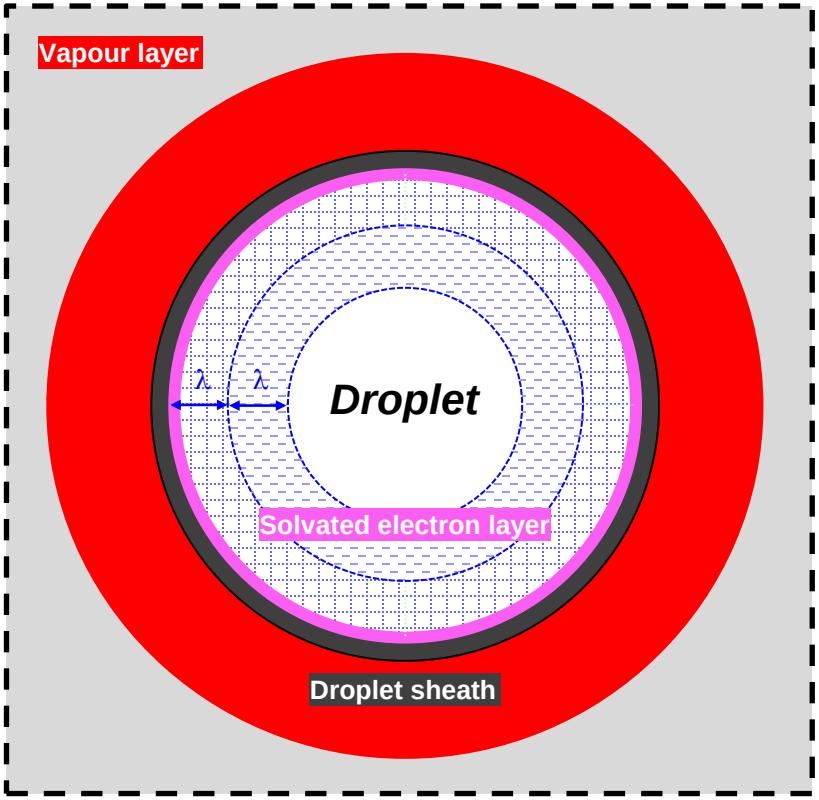

Problem

Full exponential Poisson-Boltzmann equation required. Problem for simulation.

$$n(r) = n_0 e^{+\frac{e(\phi(r)-\phi_0)}{kT}}$$

$$p(r) = p_0 e^{-\frac{e(\phi(r)-\phi_0)}{kT}}$$

Solvated electron layer

pd.maguire@ulster.ac.uk

- Debye-Huckel Theory
  - Surface electron charge
  - attracts H^+ into Debye layer λ_1 and
  - repels OH^- into Debye layer λ_2.

$$\lambda^2 = \frac{\varepsilon k_B T}{e^2 n}$$

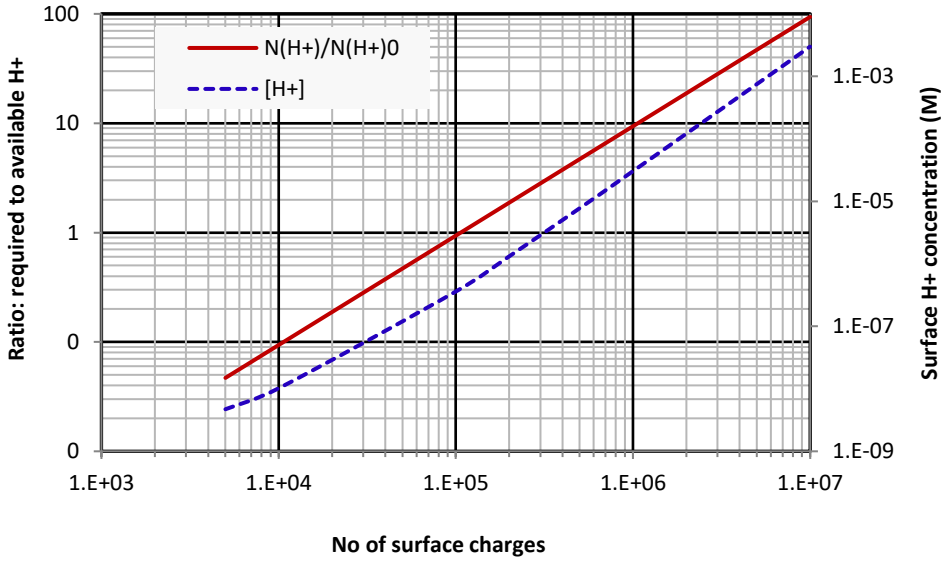

Red curve: ratio of N^*_{H+} (no of H^+ molecules required to screen surface charge Q_s.) to N_{H+} (no of H^+ molecules available)

Blue curve: N_{H+} (no of H^+ molecules available)

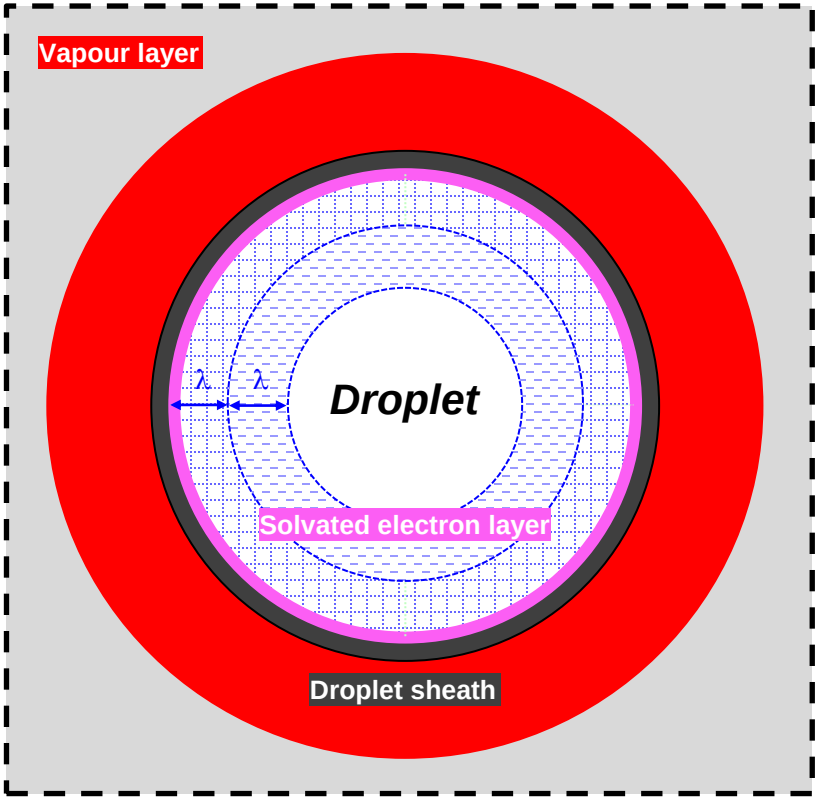

For $Q_s > 10^5 e$, $N^*_{H+}/N_{H+} > 1$

- Enhanced dissociation constant (K_a)
  - presumably further self-ionisation occurs in central region i.e. the average dissociation of water in the droplet is increased due to the charged surface.

Electron solvation

pd.maguire@ulster.ac.uk

- Solvation Energy Barrier
  - Does an energy barrier exist to electron adsorption and solvation?
  - What is the electron arrival energy?
- Electron solvation
  - excess electron in free mobile state in the solvent conduction band
  - transfers from to spatially localised state: trapped in potential well, formed by configurational changes induced by the electron itself.
  - electrons can exist in localised as well as extended (delocalised) states.
- Electron states
  - lowest energy ***extended*** state is the bottom of the liquid conduction band, normally empty in a liquid.
  - trapped state A: pre-solvated electron - may occur at a broken hydrogen bond site.
  - trapped state B: solvated electron – tetrahedral water cage arrangement
  - simplest model: free scattering electron is trapped in a pre-solvated state, in less than a picosecond, and finally solvated upon relaxation of the solvent.

Electron solvation

pd.maguire@ulster.ac.uk

- Solvation Energy Barrier
  - Does an energy barrier exist to electron adsorption and solvation?
  - What is the electron arrival energy?
- Continuum dielectric model of solvated electrons
  - solvated electron treated as a point charge at centre of a spherical cavity i.e. bound within a dielectric medium
  - trapped in the potential well formed by the polar solvent environment –
  - one O – H from each of 4 x H_2O molecules is hydrogen-bonded to the electron.
  - Born equation: solvation energy for charged species, represents work done transferring charge from gas to liquid
  - equivalent to the electrostatic energy required to charge a sphere in the liquid, with dielectric constant ε_r, relative to that required to discharge an ion in the gas.
  - more accurately: work required to polarise dielectric cavity after electron has been transferred.
  - the process of solvation results in heat release.
  - large electron solvation energy of -156 kJ mol^{-1} (or 1.617 eV per electron)
- Relaxation time
  - Solvent reorganisation, equilibrium → non-equilibrium state
  - Local equilibrium assumed – for theory

Electron solvation

pd.maguire@ulster.ac.uk

- Solvation Energy Barrier
  - Does an energy barrier exist to electron adsorption and solvation?
  - What is the electron arrival energy?
- Continuum dielectric model of solvated electrons
  - the process of solvation results in heat release.
  - large electron solvation energy of −156 kJ mol^{-1} (or 1.617 eV per electron)
- Relaxation time
  - Solvent reorganisation, equilibrium → non-equilibrium state
  - Local equilibrium assumed – for theory
- Vertical Detachment (or Binding) Energy (VDE or VBE)
  - cluster models
  - **Solvent Reorganization Energy (SRE)**: the difference in solvation free energy between nonequilibrium and equilibrium polarizations. Depends on optical permittivity.
  - **Adiabatic Electron Binding Energy (AEBE)**: difference in equilibrium solvation free energy for neutral and negatively charged cluster - depends on permittivity ε_r, cavity radius, cluster size.
  - extrapolate for bulk water, infinite cluster size.
  - VDE (water): **3.12 eV** (calculated)
  - VDE (large clusters): **3.3 eV** (experimental)
  - VDE (water droplets): **3.7 eV** (experimental)

Electron solvation

pd.maguire@ulster.ac.uk

- Solvation Energy Barrier
  - Does an energy barrier exist to electron adsorpt
  - What is the electron arrival energy?

ARTICLES
PUBLISHED ONLINE: 7 MARCH 2010 | DOI: 10.1038/NCHEM.580
nature chemistry

Binding energies, lifetimes and implications of bulk and interface solvated electrons in water

Katrin R. Siefermann[1], Yaxing Liu[1], Evgeny Lugovoy[2], Oliver Link[1], Manfred Faubel[3], Udo Buck[3],

- VDE
  - VDE (water): **3.12 eV** (calculated)
  - VDE (large clusters): **3.3 eV** (experimental), VDE (water droplets): **3.7 eV** (experimental)
- Experimental evidence
  - Siefermann et al.
  - Liquid jet photoelectron spectroscopy (PES)
  - measured VDE of surface partially solvated electrons: **1.6 eV**.
  - similar to VDE of amorphous solid water (1.4 eV).
  - penetration depth: **less than one monolayer**
  - significant free-energy barrier may exist between surface and bulk solvation
  - due to molecular reorientation of surface water mediated by surface-bound electrons preventing penetration of surface electrons into the bulk.
  - free-energy barrier height estimate **~ 0.2 eV – 0.5 eV.**
- Simulations
  - simulations have been unable to find such a barrier
  - capability of PES to distinguish interfacial from bulk electrons is questioned.

Electron solvation

pd.maguire@ulster.ac.uk

- Solvation Energy Barrier
  - Does an energy barrier exist to electron adsorption and solvation?
  - What is the electron arrival energy?
- VDE
  - VDE (water): **3.12 eV** (calculated)
  - VDE (large clusters): **3.3 eV** (experimental),
  - VDE (water droplets): **3.7 eV** (experimental)
- Experimental evidence
  - measured VDE of surface partially-solvated electrons: **1.6 eV**.
  - penetration depth: **less than one monolayer**
  - free-energy barrier height estimate **~ 0.2 eV – 0.5 eV.**
- Electron net arrival energy at droplet
  - when droplet at floating potential, ϕ.
  - only electrons with $E > \phi$. will reach droplet.
  - from EEDF, $n_e(E > \phi) \cong n_e(E = \phi + \Delta\phi)$
  - net arrival energy $\Delta\phi \sim 0$
  - **lower than estimated solvation barrier height.**

Electron solvation

pd.maguire@ulster.ac.uk

- Solvation Energy Barrier
  - Does an energy barrier exist to electron adsorption and solvation?
  - What is the electron arrival energy?
- Experimental evidence
  - penetration depth: **less than one monolayer**
  - free-energy barrier height estimate **~ 0.2 eV – 0.5 eV.**
- Electron net arrival energy at droplet
  - net arrival energy $\Delta\phi \sim 0$
  - **lower than estimated solvation barrier height.**
- Estimates from plasma - bulk liquid
  - *Rumbach et al., Nature Comms* **6**, 7248 (2015) Planar plasma – bulk liquid studies:
  - Solvated electron concentration – approaching **1 mM**. *Estimate.*
  - Electron penetration depth **10 nm**
  - **Electron arrival energy**: sheath electric field, sheath width vs mean free path, collisions
  - Ion energy simulations with collisions: 6 – 10 eV (DBD or single filaments) Babaeva 2012, 2 – 3 eV (APPJ) Babaeva 2020, < 1 eV (90%), 1 – 8 eV (10%) (DC microplasma) Choi 2007, 5 – 12 eV Gopalakrishnan 2016

Solvated electron monolayer

pd.maguire@ulster.ac.uk

- Solvation Energy Barrier
  - Does an energy barrier exist to electron adsorption and solvation?
  - What is the electron arrival energy?
- Experimental evidence
  - penetration depth: **less than one monolayer**
  - free-energy barrier height estimate **~ 0.2 eV – 0.5 eV.**
- Electron net arrival energy at droplet
  - net arrival energy $\Delta\phi \sim 0$
  - **lower than estimated solvation barrier height.**
- Solvated electron monolayer
  - Q = Rayleigh charge
  - Minimum electron – electron distance: **10 nm**
  - Solvation cavity diameter / gyration diameter: **0.5 nm**
  - Concentration: up to **20 mM**
  - $e_{aq}^- + e_{aq}^- + 2H_2O \rightarrow H_2 + 2OH^-$ (R1)

Plasma versus Radiolysis or e-Beam

pd.maguire@ulster.ac.uk

- X 10^3 – 10^7 faster
  - **Similar dose rate as gamma radiation**
- Plasma-droplet
  - Dose rate assuming **x%** plasma energy delivered to drop according to ratio VOL_{drop} / VOL_{plasma}
  - 5×10^{-2} kGy s^{-1}.
- Solvated Electron Reduction Hypothesis
  - Reactions: 2nd order
  - Droplet negatively charged
  - **Electrons arrive with very low energy**
  - **Electrostatically confined**
  - **shallow surface layer**
  - Very high local concentration

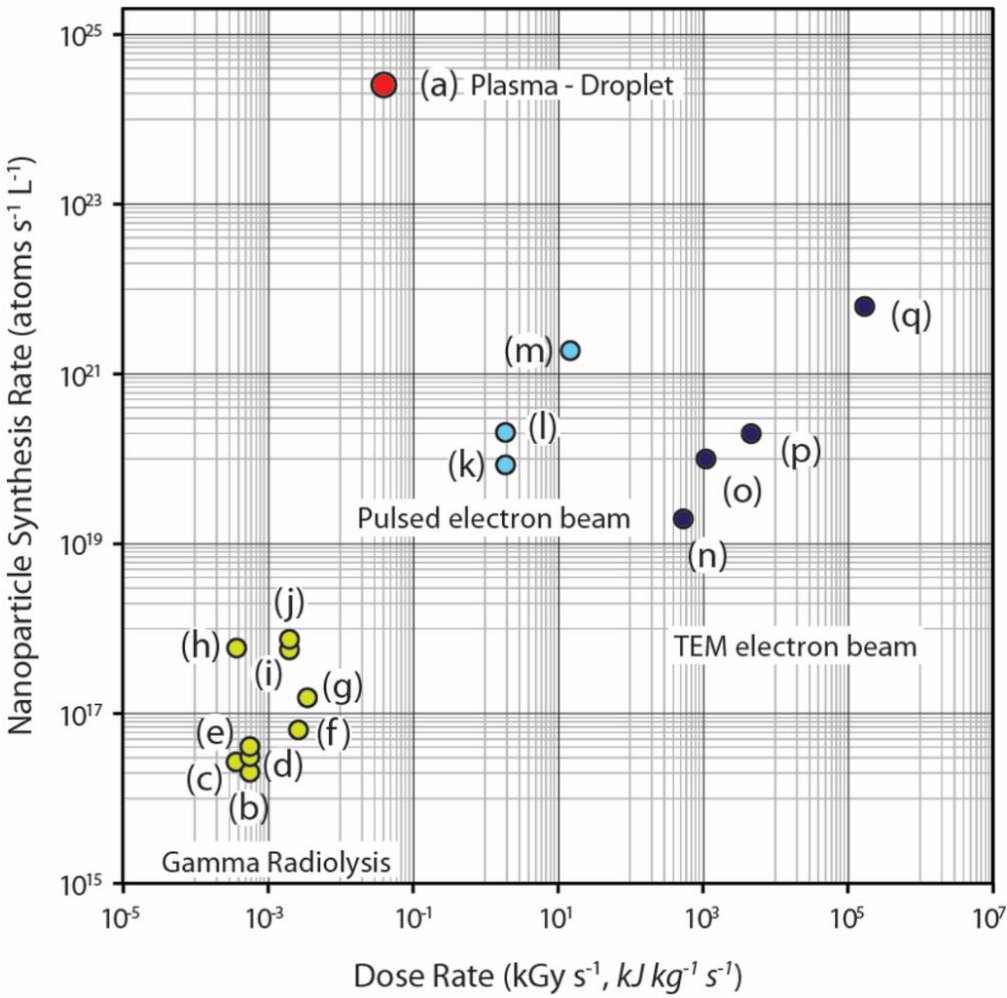

$HAuCl_4$. The reduction of **Au^{III}** proceeds via reactions as:

II	$Au^{III}Cl_4^- + e_{aq}^- \rightarrow Au^{II}Cl_4^{2-}$	(R1)
III / I	$2\ Au^{II}Cl_4^{2-} \rightarrow Au^{III}Cl_4^- + Au^{I}Cl_2^- + 2Cl^-$	(R2a)
0	**$Au^{I}Cl_2^- + e_{aq}^- \rightarrow Au^{0}Cl_2^{2-}$**	**(R3)**
I / II	$Au^{III} + Au^0 \rightarrow Au^{I}$ and Au^{II}	(R4)

Continuous In-Flight Synthesis for On-Demand Delivery of Ligand-Free Colloidal Gold Nanoparticles, Maguire et al., Nano Letts., 2017, https://dx.doi.org/10.1021/acs.nanolett.6b03440

Funding Sources

EPSRC
Pioneering research and skills

THE ROYAL SOCIETY

National Science Foundation
WHERE DISCOVERIES BEGIN

Department for Employment and Learning
www.delni.gov.uk

The Leverhulme Trust

sfi Science Foundation Ireland

European Union
European Regional Development Fund
Investing in your future

JAPAN SOCIETY FOR THE PROMOTION OF SCIENCE · FOUNDED 1932

Invest Northern Ireland

MARIE CURIE ACTIONS

NATO OTAN

University of Glasgow

Declan Diver
Hugh Potts
Euan Bennet

University of St Andrews

RUB
RUHR-UNIVERSITÄT BOCHUM

NUI Galway
OÉ Gaillimh

Queen's University Belfast

University of Glasgow

UNIVERSITY OF CAMBRIDGE

SCRIPPS INSTITUTION OF OCEANOGRAPHY UC San Diego

National Institute of Advanced Industrial Science and Technology (AIST)
独立行政法人　産業技術総合研究所

NATO
SfP 984555